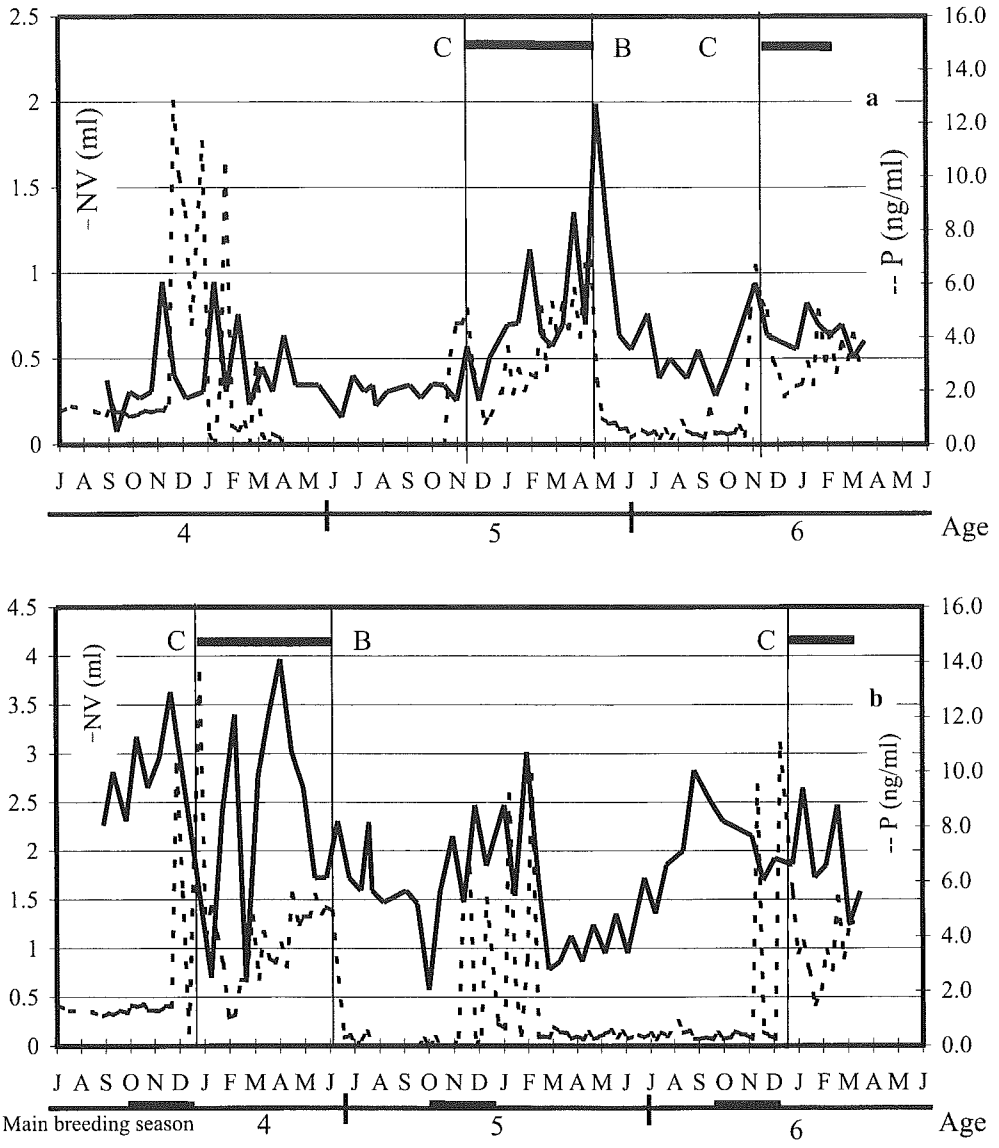

Fig. 9a, b Two examples showing the relationship between the age changes in NV (*solid line*) and the secretion profile of progesterone (*dotted line*). **a** Number 1433; **b** number 1447. *C* (estimated conception), *B* (parturition), and the *thick line* (pregnancy) delineate pregnancy-related changes

P followed almost exactly the change in NV from conception to parturition, but the secretion of P ceased from just after parturition until the next breeding season.

The infant of subject 1469 suckled from its mother for more than 1 year after birth, and the NV graph of this subject increased substantially (Fig. 6). In contrast, the other four subjects in Fig. 6 exhibited the same cycle in the 7th year of life as that found in the previous year. Thus, although NV appeared to increase due to suckling, the exact effect of suckling, especially the cumulative effect, on NV is left for future study.

Discussion

Development and seasonality of the testis in Japanese macaques

The outline of testicular development in Japanese macaques is as follows: the testis starts its rapid increase in size at puberty during the breeding season when animals are about 4.5 years old (e.g. Nigi et al. 1980; Matsubayashi and Mochizuki 1982). There is considerable variation with locality (Hamada et al. 1986) and nutritional status (Hamada et al. 1999) but, on the whole, the testis matures at about 10 years of age (Matsubayashi and Mochizuki 1982). Although the number of subjects was limited, TV did not show age-related changes after reaching maturation. Some animals that grew faster than average in physical dimensions (e.g., body weight) were precocious and showed a small temporal TV increase 1 year earlier. Male long-tailed macaques show a tendency of "catch-up" testicular development, that is, the later the testis starts pubertal development, the faster it develops (Meussy-Dessolle and Dang 1985). We did not, however, find any such significant "catch-up" in the present study.

The TV in Japanese macaques shows a strict seasonality, with an increase before and during the breeding season and a rapid decrease at the end of the season. The

first TV peak at puberty is significantly smaller than those that occur thereafter. The amplitude of seasonal cyclicity and baseline volume becomes higher as animals mature. The concentration of T increases from 4 to 7 years with considerable fluctuation due to seasonality. Individual variation is substantial in terms of age at T peak and TV peak but, as the cyclicity and amplitude correspond closely among individuals, the cross-sectional diagram preserves the seasonal effect (Fig. 1b).

The relationship between TV and T level was quite tight in each of the individuals, but there was a slight lag between T peak and TV increase in the period where TV had not yet attained maturity (see Fig. 4). Matsubayashi and Enomoto (1983) reported for adult Japanese macaques that the T level increases rapidly from July to attain a peak in September, and that the TV peak is found in October. Their result appears to show a lag between T secretion and TV increase, but this may reflect their measurement schedule. Whereas they measured T monthly, TV was measured only four times a year (April, July, October, and January). The time lag between TV increase and T secretion in immature individuals is quite different from that between the frequency of breeding behaviors (mounts) and T secretion (Rostal et al. 1986).

The presence of cycling females has been reported to influence males sharing the same environment (Vandenbergh 1969). We found that males in the same cage tended to show similar profiles, and, notably, cycling females were also reared in these cages. We could not, however, substantiate any such influence in this study (see pp 389–392 in Dixson 1998).

Development and seasonality in the nipple size of Japanese macaques

Nipple size variation in macaques has not attracted much attention, though there are studies that deal with nipple preference (laterality, e.g. Tanaka 1989). The size varies widely among individuals because there are many factors influencing it: growth, reproductive maturation, menstrual cycle, physical factors such as suckling by offspring, pregnancy and parturition, lactation, and aging. In the peri-adolescent period, the age change in nipple size appears consistent.

The nipple in Japanese macaques starts to grow rapidly at about 3.5 years of age, in conjunction with other characters that advertise reproductive state (the swelling of sexual skin and reddening of the face and sexual skin). The Japanese macaque subjects showed substantial P secretion in their fourth winter (ca. 3.5 years of age), indicating that they may have commenced their menstruation cycles, and their NV increased accordingly over the fourth summer and autumn. Therefore, it seems that many of them experienced menarche in the autumn and, a few months later, their first ovulation. In the case of rhesus macaques (Terasawa et al. 1983), the period between menarche (30.7 ± 1.2 SE months of age) and first ovulation (48.1 ± 2.2 SE months of age) is much longer than that in Japanese macaques.

The nipples finally mature at around 7 years of age in Japanese macaques (5–10 years, the latter half of adolescence and the young-adult period). Seasonality in NV was evident in every female analyzed longitudinally where there was a peak in the breeding season (winter) and a trough in the delivery season (spring). In contrast to the testis, seasonality in NV, starting from puberty, was not evident in the cross-sectional data analysis because of wide individual variation. Throughout the adult period, from 10 to 25 years of age, NV seems to be consistent, though there may be seasonal fluctuation and a cumulative effect of being suckled by offspring in adult macaques, but these are topics for future study. In general, NV gradually decreases from 25 years of age, when, on average, the post-menopausal period begins (Takahata et al. 1995; Pavelka and Fedigan 1999).

The NV in many individuals correlates strongly with changes in reproductive physiology as represented by the P concentration profile in this study. Thus the NV follows the menstrual cycle, and its peak precedes the P peak by about 2 weeks (the mid-follicular phase). The menstrual cycle is often characterized by the concentration profiles of E2, gonadotropins (LH and FSH), and P (Dixson 1998), and the fact that the NV peak is found in the mid-follicular phase indicates that E2 is the major hormone influencing nipple enlargement. A close relationship has been reported between the E2 level and nipple size in rhesus macaques (Terasawa et al. 1983). Nevertheless, there also exists the possibility that other hormones are also involved.

The combination effect of P and E2 on nipples is worth considering even though Terasawa et al. (1983) found no relationship between P and NV before ovulation in the peri-pubertal phase. In the luteal phase P is secreted mainly in preparation for pregnancy (e.g. synthesis of secretory material by uterine glands, Johnson and Everitt 1995; cellular differentiation in the uterus, Baulieu 1992), and both E2 and P are considered to function in maintaining the increase of NV. In the breeding season, when several menstrual cycles occur, the average NV remains higher than that in the non-breeding season. This difference may be due to the fact that the regular secretion of many hormones, including E2 and P, keeps the nipples large throughout the breeding season. The combination effect of P and E2 is also found in the change of NV during pregnancy. After conception, both P and E2 are secreted and the change in NV parallels the concentration profile of P. It is known that P is an antagonist of mineralocorticoids, causing water retention (Felig et al. 1995). The two hormones, E2 and P, in conjunction with others, influence the breasts of women in the luteal phase (Johnson and Everitt 1995), so their combined effect may influence the nipples in Japanese macaques.

The other pattern of NV change that must be explained is that NV increased in some subjects in the

non-breeding season, from spring to autumn. We suspected that a non-ovulatory menstrual cycle caused this increase. Such cycles have been reported for subjects reared in indoor cages with a relatively high frequency (Nozaki 1991). However, as the subjects for the present study were reared in a cage with an outdoor enclosure, it seems an unlikely explanation. Mori et al. (1997) reported on food-enhanced perineal swelling in Japanese macaques in poor nutritional condition, but, although reproductive state is known to relate closely to nutritional condition (Nigi et al. 1995; Nigi and Morimitsu 1997), it could not be used as an explanation in this case. This, then, is also a subject for future study.

The relationship between NV change and social life

It is widely known that Japanese macaques have a multimale, multi-female type of society and will not make "fission and fusion" as chimpanzees do (e.g. Melnick and Pearl 1987), and they are always attentive to the behavior of other members, such as posture and all kinds of facial and tail movements, however slight. It follows then, that they probably also recognize morphological changes in other individuals. The morphological changes related to reproduction, such as sexual swelling, reddening of the facial and sexual skins, and enlargement of testes and nipples, would function as visual cues. Although NV varies considerably among individuals, the present study showed that changes in a given individual due to seasonality and the menstrual cycle are great enough to be detected by other troop members. Humans familiar with subject macaques can also detect the change. Japanese macaques tend to sit keeping their torsos erect, and this posture ensures that the nipples are visible to other members. Nipples appear to advertise secondarily the reproductive state of an individual, together with the remarkable advertisement found in the anogenital region and the caudal aspects of the thigh that are obscured when the individual sits. The present study suggests that peak NV occurs in the midfollicular phase, that is, about 1 week earlier than ovulation. This pattern is similar to that of the sexual swelling in chacma baboons (Bielert 1986), where the skin swells in the follicular phase and starts to break down around the day of ovulation, and frequent ejaculate is observed around the late follicular phase. As Japanese macaques have keen vision, and reddish nipples contrast sharply against their whitish chest, other troop members can detect the nipple change and respond appropriately.

Nipple size has often been used by human observers to classify adult females as either parous or nulliparous for the determination of population structure with considerable accuracy (H. Ohsawa, personal communications). It is also possible for human observers to determine whether the individual is lactating or not simply by observing the nipples. It is, therefore, thought that macaques can also discriminate that difference. We have yet, however, to elucidate the exact relationship between size changes in nipples and behavioral changes in other individuals.

Acknowledgements We thank the staff of the section of Morphology and the Center for Human Evolution Modeling Research of the Primate Research Institute, Kyoto University, for their help and valuable suggestions. This research was supported by a grant-in-aid for COE Research 2001, a grant-in-aid for Specially Promoted Research (COE) 2002, and grants-in-aid nos. 11833008, 11304059, and 14204083 from the Ministry of Education, Culture, Sports, Science and Technology.

References

Baulieu E-E (1992) Hormones: from molecules to disease. Chapman and Hall, New York

Bielert C (1986) Sexual interactions between captive adult male and female Chacma baboons (*Papio ursinus*) as related to the female's menstrual cycle. J Zool (Lond) 209:521–536

Dixson AF (1998) Primate sexuality. Oxford University Press, Oxford

Felig P, Baxter JD, Frohman LA (1995) Endocrinology and metabolism, 3rd edn. McGraw-Hill, New York

Glick BB (1979) Testicular size, testosterone level, and body weight in male *Macaca radiata*. Folia Primatol 32:268–289

Hamada Y, Hayakawa S, Suzuki J, Ohkura S (1999) Adolescent growth and development in Japanese macaques (*Macaca fuscata*): punctuated adolescent growth spurt by season. Primates 40:439–452

Hamada Y, Hayakawa S, Suzuki J, Watanabe K, Ohkura S (2003) Body fat and its seasonality in Japanese macaques (*Macaca fuscata*). Mamm Study 28:79–88

Hamada Y, Iwamoto M, Watanabe T (1986) Somatometrical features of Japanese monkeys in the Koshima Islet: in viewpoint of somatometry, growth, and sexual maturation. Primates 27:471–484

Hamada Y, Watanabe T, Iwamoto M (1996) Physique Index for Japanese macaques (*Macaca fuscata*): age change and regional variation. Anthropol Sci 104:305–323

Hazama N (1964) Weighing wild Japanese monkeys in Arashiyama. Primates 5(3–4):81–104

Johnson MH, Everitt BJ (1995) Essential reproduction, 4th edn. Blackwell, Oxford

Knobil E, Hotchkiss J (1988) The menstrual cycle and its neuroendocrine control. In: Knobil E, Neill J (eds) The physiology of reproduction, vol 2. Raven, New York, pp 1971–1994

Malina RM, Bouchard C (1991) Growth, maturation, and physical activity. Human Kinetics, Champaign, Ill.

Marson J, Meuris S, Cooper RW, Jouannet P (1991) Puberty in the male chimpanzee: progressive maturation of semen characteristics. Biol Reprod 44:448–455

Mastroianni L, Coutifaris C (1990) Reproductive physiology. In: Rosenfield A, Fathalla MF (eds) The FIGO manual of human reproduction, vol 1. Parthenon, New Jersey

Matsubayashi K, Enomoto T (1983) Longitudinal studies on annual changes in plasma testosterone, body weight and spermatogenesis in adult Japanese monkeys (*Macaca fuscata fuscata*) under laboratory conditions. Primates 24:521–529

Matsubayashi K, Mochizuki K (1982) Growth of male reproductive organs with observation of their seasonal morphlogic changes in the Japanese monkey (*Macaca fuscata*). Jpn J Vet Sci 44:891–902

Melnick DJ, Pearl MC (1987) Cercopithecines in multimale groups: genetic diversity and population structure. In: Smuts BB, Cheney DL, Seyfarth RM, Wranghan RW, Struhsaker TT (eds) Primates societies. University of Chicago Press, Chicago, pp 121–134

Meussy-Dessolle N, Dang DC (1985) Plasma concentration of testosterone, dihydrotestosterone, Δ4-androstenediore, dehydroepiandrosterone and oestradiol-17β in the crab-eating monkeys (*Macaca fascicularis*) from birth to adulthood. J Reprod Fertil 74:347–359

Mori A, Yamguchi N, Watanabe K, Shimizu K (1997) Sexual maturation of female Japanese macaques under poor nutritional conditions and food-enhanced perineal swelling in the Koshima Troop. Int J Primatol 18:553–579

Nigi H, Morimitsu Y, Hayama S (1995) Correlation between pregnancies and fats accumulated in great omentum in the free-ranging Japanese monkeys (in Japanese). Primate 11:291

Nigi H, Morimitsu Y (1997) Correlation between reproductive success and fats accumulated in greater omemtum in the free-ranging female Japanese monkeys at Takasakiyama (in Japanese). Primate Res 13:236

Nigi H, Tiba T, Yamamoto S, Floescheim Y, Ohsawa N (1980) Sexual maturation and seasonal changes in reproductive phenomena of male Japanese monkeys (*Macaca fuscata*) at Takasakiyama. Primates 21:230–240

Nozaki M (1991) Mechanisms controlling seasonal breeding in Japanese monkeys (in Japanese with English abstract). Primate Res 7:103–125

Nozaki M (1994) Mechanisms controlling the seasonal breeding of Japanese monkeys (in Japanese with English abstract). J Reprod Dev 40(6):j105–j115

Pavelka MSM, Fedigan LM (1999) Reproductive termination in female Japanese monkeys: a comparative life history perspective. Am J Phys Anthropol 109:455–464

Primate Research Institute (2003) Guide for the care and use of laboratory primates. Primate Research Institute, Kyoto University http://www.pri.kyoto-u.ac.jp/index.html

Rostal DC, Glick BB, Eaton GG, Resko JA (1986) Seasonality of adult male Japanese macaques (*Macaca fuscata*): androgens and behavior in a confined troop. Horm Behav 20:452–462

Sade DS (1964) Seasonal cycle in size of testes of free-ranging *Macaca mulatta*. Folia Primatol 2:171–180

Suzuki J, Ohkura S, Hayakawa S, Hamada Y (2000) Time series analysis of plasma insulin-like growth factor-I and gonadal steroids in adolescent Japanese macaques (*Macaca fuscata*). J Reprod Dev 46:157–166

Takahata Y, Koyama N, Suzuki S (1995) Do the old aged females experience a long post-reproductive life span? The cases of Japanese macaques and chimpanzees. Primates 36:169–180

Tanaka I (1989) Change of nipple preference between successive offspring in Japanese macaques. Am J Primatol 18:321–325

Tanner JM (1962) Growth at adolescence. 2nd edn. Blackwell, Oxford

Terasawa E, Nass TE, Yeoman RR, Loose MD, Schultz NJ (1983) Hypothalamic control of puberty in the female rhesus macaque. In: Norman RL (ed) Neuroendocrine aspects of reproduction: ORPRC symposia on primate reproduction bilogy. Academic, New York, pp 149–182

Vandenbergh JG (1969) Endocrine coordination in monkeys: male sexual responses to the female. Physiol Behav 4:261–264

The EMBO Journal (2004) 23, 1889–1899 | © 2004 European Molecular Biology Organization | All Rights Reserved 0261-4189/04
www.embojournal.org

THE EMBO JOURNAL

JNK promotes Bax translocation to mitochondria through phosphorylation of 14-3-3 proteins

Fuminori Tsuruta[1], Jun Sunayama[1], Yasunori Mori[1], Seisuke Hattori[2], Shigeomi Shimizu[3], Yoshihide Tsujimoto[3], Katsuji Yoshioka[4], Norihisa Masuyama[1] and Yukiko Gotoh[1,5,*]

[1]Institute of Molecular and Cellular Biosciences, University of Tokyo, Yayoi, Bunkyo-ku, Tokyo, Japan, [2]Division of Cellular Genome Proteomics, Institute of Medical Science, University of Tokyo, Shirokanedai, Minato-ku, Tokyo, Japan, [3]Department of Post-Genomics & Disease, Osaka University Graduate School of Medicine, Yamadaoka, Suita, Osaka, Japan, [4]Division of Cell Cycle Regulation, Cancer Research Institute, Kanazawa University, Takara-machi, Kanazawa, Japan and [5]PRESTO Research Project, Japan Science and Technology Corporation, Tokyo, Japan

Targeted gene disruption studies have established that the c-Jun NH_2-terminal kinase (JNK) is required for the stress-induced release of mitochondrial cytochrome *c* and apoptosis, and that the Bax subfamily of Bcl-2-related proteins is essential for JNK-dependent apoptosis. However, the mechanism by which JNK regulates Bax has remained unsolved. Here we demonstrate that activated JNK promotes Bax translocation to mitochondria through phosphorylation of 14-3-3, a cytoplasmic anchor of Bax. Phosphorylation of 14-3-3 led to dissociation of Bax from this protein. Expression of phosphorylation-defective mutants of 14-3-3 blocked JNK-induced Bax translocation to mitochondria, cytochrome *c* release and apoptosis. Collectively, these results have revealed a key mechanism of Bax regulation in stress-induced apoptosis.

The EMBO Journal (2004) **23,** 1889–1899. doi:10.1038/sj.emboj.7600194; Published online 8 April 2004
Subject Categories: differentiation & death
Keywords: apoptosis; Bax; JNK; phosphorylation; 14-3-3

Introduction

Apoptosis is essential for normal development and maintenance of tissue homeostasis. Disruption of the equilibrium between pro- and anti-apoptotic factors results in pathological conditions such as cancer, autoimmune disease and neurodegenerative disorders (Krammer, 2000; Yuan and Yankner, 2000). The loss of mitochondrial membrane integrity and the consequent release of cytochrome *c* into the cytosol are important events during apoptosis and are regulated by the Bcl-2 family of proteins (Wang, 2001). As the members of the Bcl-2 family exert their actions mostly at the level of mitochondria and reside upstream of the onset of irreversible cellular damage, they play a pivotal role in determining whether a cell will live or die (Gross *et al*, 1999; Tsujimoto and Shimizu, 2000). All Bcl-2 family members possess at least one of four conserved motifs known as Bcl-2 homology domains (BH1–BH4). Most anti-apoptotic members, including Bcl-2 and Bcl-x_L, contain all the four domains. Pro-apoptotic members such as Bax and Bak lack the BH4 domain, whereas other pro-apoptotic members, the so-called BH3 domain-only proteins that include Bid, Bim and Bad, contain only the BH3 domain (Gross *et al*, 1999; Tsujimoto and Shimizu, 2000).

Recently, it has been demonstrated that Bax plays an essential role in inducing apoptosis in response to stress stimuli, as revealed by gene disruption of Bax and of Bax and Bak (Knudson *et al*, 1995; Lindsten *et al*, 2000; Wei *et al*, 2001; Zong *et al*, 2001). Bax is localized mostly in the cytoplasm, but redistributes to mitochondria in response to stress stimuli (Hsu *et al*, 1997; Wolter *et al*, 1997). After translocation to mitochondria, Bax induces cytochrome *c* release either by forming a pore by oligomerization in the outer mitochondrial membrane, or by opening other channels (Shimizu *et al*, 1999; Saito *et al*, 2000; Kuwana *et al*, 2002). The mechanisms underlying Bax translocation, however, are not fully understood.

Recent studies have shown that several proteins including 14-3-3 proteins prevent apoptosis through sequestration of Bax (Samuel *et al*, 2001; Guo *et al*, 2003; Nomura *et al*, 2003; Sawada *et al*, 2003). 14-3-3 proteins, which include seven isoforms in humans, are also implicated in antagonizing apoptotic signals through association with other pro-apoptotic proteins such as Bad, FKHRL1, ASK1 and Nur77 (Zha *et al*, 1996; Datta *et al*, 1997; Brunet *et al*, 1999; Zhang *et al*, 1999; Masuyama *et al*, 2001; van Hemert *et al*, 2001; Yaffe, 2002). Most 14-3-3 target proteins require phosphorylation to interact with 14-3-3, and consensus phosphoserine containing 14-3-3 binding motifs (RSXpSXP and RXXXpSXP) have been defined (Muslin *et al*, 1996; Yaffe *et al*, 1997). On the other hand, there are several examples of proteins containing dramatic variations from these motifs, including some that do not even require phosphorylation for binding, such as exoenzyme S, the platelet glycoprotein IB-IX-V complex, the plasma membrane H^+-ATPase AHA2 and *Drosophila* PAR-1 (Du *et al*, 1996; Masters *et al*, 1999; Svennelid *et al*, 1999; Benton *et al*, 2002). Bax also interacts with 14-3-3 proteins in a phosphorylation-independent manner (Nomura *et al*, 2003). A substantial proportion of Bax molecules is bound to 14-3-3 proteins in the cytosol of healthy cells; in response to stress stimuli, however, Bax dissociates from 14-3-3 and redistributes to mitochondria (Nomura *et al*, 2003). Moreover, caspases activated by stress stimuli cleave 14-3-3θ within its COOH-terminal region and promote its dissociation from Bax (Nomura *et al*, 2003). These observations are consistent with previous results showing that disruption of the 14-3-3σ gene promotes Bax translocation to mitochondria in response to cellular stresses (Samuel *et al*, 2001). However,

*Corresponding author. Institute of Molecular and Cellular Biosciences, University of Tokyo, 1-1-1 Yayoi, Bunkyo-ku, Tokyo 113-0032, Japan. Tel.: +81 3 5841 8473 or 7859; Fax: +81 3 5841 8472; E-mail: ygotoh@iam.u-tokyo.ac.jp

Received: 16 September 2003; accepted: 8 March 2004; published online: 8 April 2004

the translocation of Bax to mitochondria occurs independently of caspase activation in a number of systems (Putcha *et al*, 1999; Gilmore *et al*, 2000; Tsuruta *et al*, 2002), suggesting the existence of another mechanism responsible for the dissociation of Bax from 14-3-3 proteins.

The c-Jun N-terminal kinase (JNK) represents a group of mitogen-activated protein kinases (MAPKs), which is activated when cells are exposed to environmental stresses (Davis, 2000). In all, 10 members of the JNK family are generated by the alternative splicing of transcripts derived from the JNK1, JNK2 and JNK3 genes. The studies of JNK gene disruption in mice have confirmed that JNK contributes to stress responses (Davis, 2000). JNK3 is essential for apoptosis of hippocampal neurons following exposure to excitotoxic stresses (Yang *et al*, 1997). JNK1 and JNK2 are required for apoptosis of thymocytes in response to ligation of the T-cell receptor and of neurons in the developing hindbrain (Kuan *et al*, 1999; Sabapathy *et al*, 2001). Furthermore, JNK1 and JNK2 double-knockout cells are resistant to apoptosis induced by UV, anisomycin or DNA damage (Tournier *et al*, 2000). Moreover, recent studies have shown that Bax and Bak are required for JNK-induced apoptosis, and that Bax remains inactive upon exposure of JNK-deficient fibroblasts to environmental stress (Lei *et al*, 2002). How then does JNK activate Bax?

In this study, we show that 14-3-3ζ and 14-3-3σ are direct targets of JNK and that phosphorylation of 14-3-3 proteins by JNK results in dissociation of Bax from 14-3-3 proteins, leading to apoptosis. This novel function of JNK may provide the missing link between the stress-activated kinase cascade and Bax translocation to mitochondria, a critical step in the regulation of apoptosis.

Results

Active JNK promotes Bax translocation to the mitochondria

We first examined whether JNK activation is sufficient to promote Bax translocation to the mitochondria in COS-1 cells, since Bax has been reported to be required for JNK-induced apoptosis in mouse embryonic fibroblasts (Lei *et al*, 2002). To this end, we utilized a green fluorescent protein (GFP)–Bax fusion construct to monitor Bax localization in real time (Tsuruta *et al*, 2002). In all the experiments with GFP–Bax, p35, a pan-caspase inhibitor, was co-transfected to block caspase activation induced by overexpression of GFP–Bax. As a constitutively active form of JNK, we used a fusion protein (MKK7–JNK) in which MKK7α1 and JNK1β1 are connected by the Flag epitope tag (Figure 1A); in this construct, which is similar to the one used by Lei *et al* (2002), MKK7 phosphorylates and activates JNK1 intramolecularly (K Yoshioka, unpublished data). We found that expression of MKK7–JNK (wild type, WT) promoted GFP–Bax translocation to the mitochondria (Figure 1B and C). In contrast, the fusion construct of MKK7α1 and a kinase negative JNK (MKK7–JNK (KN)) had no effect on GFP–Bax localization (Figure 1B and C), suggesting that JNK promotes Bax translocation by phosphorylation of some target(s). To determine if JNK activity triggers translocation of the endogenous Bax protein, the distribution of endogenous Bax was assessed by subcellular fractionation after transfection of COS-1 cells with the MKK7–JNK constructs. The amount of endogenous Bax detected in the mitochondrial fraction was increased, and that detected in the cytosolic fraction was decreased, by expression of MKK7–JNK(WT) but not by that of MKK7–JNK(KN). On the other hand, the abundance of the mitochondrial marker F_0F_1-ATPase subunit α (or that of the cytosolic marker α-tubulin) in the corresponding fraction was unaffected by the expression of either construct (Figure 1D). Although expression of MKK7–JNK(WT) resulted in the activation of caspase-3 in COS-1 cells (Supplementary Figure 1) (Lei *et al*, 2002), coexpression of p35, which prevented caspase-3 activation by MKK7–JNK(WT) (Supplementary Figure 1), failed to inhibit Bax translocation to the mitochondrial fraction (Figure 1D), suggesting that MKK7–JNK(WT) promoted the translocation of endogenous Bax to mitochondria independently of caspase activation.

To determine whether JNK activity is required for stress-induced translocation of Bax to the mitochondria, we examined the effect of SP600125, a JNK inhibitor, on GFP–Bax redistribution induced by the protein synthesis inhibitor anisomycin. Inhibition of protein synthesis by anisomycin triggers apoptosis in a broad variety of cells. Treatment of COS-1 cells with anisomycin resulted in phosphorylation of the JNK substrate c-Jun, and pretreatment with SP600125 blocked this effect of anisomycin (Figure 2A). Anisomycin also induced a gradual redistribution of GFP–Bax to mitochondria, and this effect of anisomycin was inhibited by SP600125 (Figure 2B). We also measured Bax translocation to the mitochondria using subcellular fractionation and found that SP600125 inhibited the translocation of endogenous Bax to mitochondria in response to treatment with anisomycin (Supplementary Figure 2). The concentration of SP600125 required for the inhibition of Bax translocation was the same as that required for the inhibition of c-Jun phosphorylation (data not shown). To verify that the effect of SP600125 was specific for JNK, we also used the JNK-binding domain peptide (JBD) (Dickens *et al*, 1997) and a dominant-negative (DN) JNK to block JNK activity. The JBD blocked anisomycin-induced GFP–Bax translocation (Figure 2C) and expression of DN form of JNK blocked GFP–Bax translocation induced by staurosporine (Supplementary Figure 3), another agent known to induce apoptosis. Taken together, these results suggest that JNK activity is required for Bax translocation to the mitochondria induced by anisomycin or by staurosporine.

JNK can regulate Bax localization independently of c-Jun, Akt and Bim

We first tested the ability of JNK to phosphorylate Bax and found that Bax is not phosphorylated by JNK in an *in vitro* kinase assay (Supplementary Figure 4). We therefore hypothesized that there is another JNK target that regulates Bax localization in response to stress stimuli. Apoptosis induced by neurotrophic factor deprivation in sympathetic neurons is mediated by the JNK-catalyzed phosphorylation of c-Jun (Harris and Johnson, 2001; Putcha *et al*, 2001; Whitfield *et al*, 2001). We examined whether c-Jun phosphorylation is required for Bax translocation to the mitochondria. MKK7–JNK(WT) phosphorylated c-Jun and induced activation of c-Jun-dependent transcription, as measured by a luciferase reporter gene controlled by an AP-1-dependent promoter (which monitors the activity of the Jun–Fos complex).

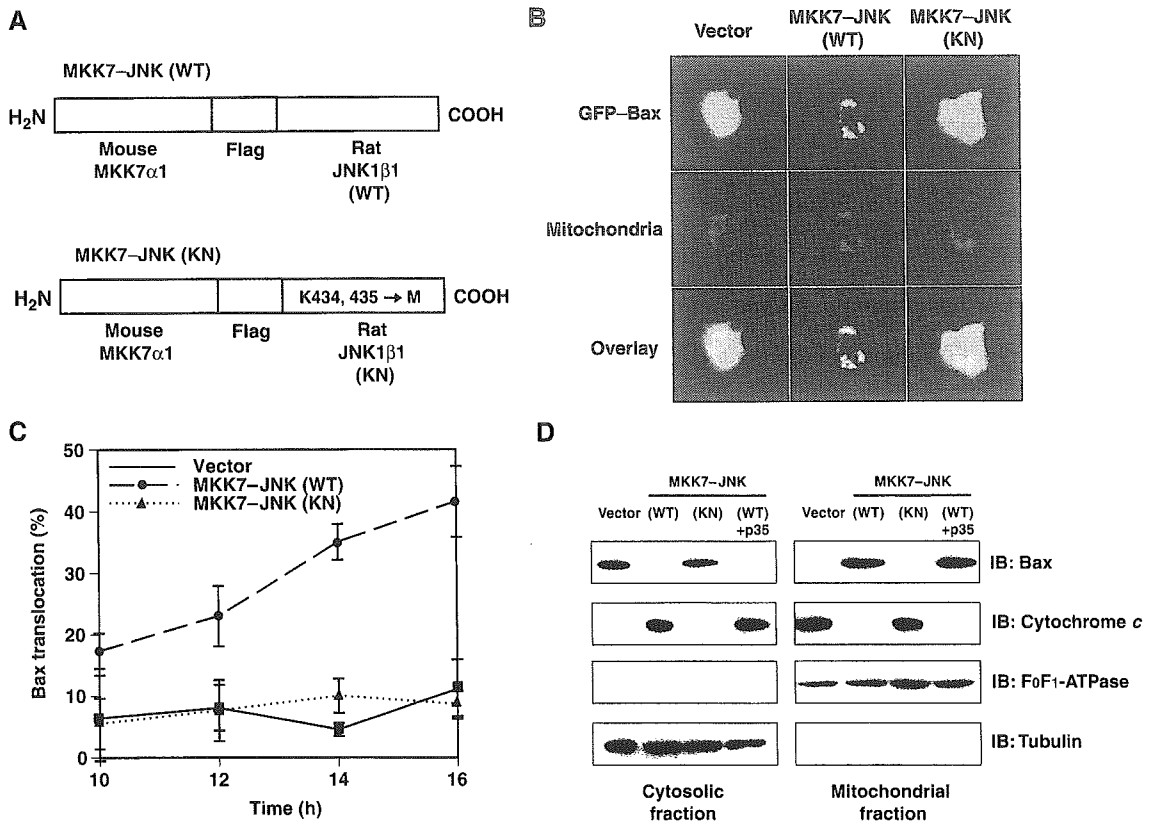

Figure 1 Expression of active JNK promotes Bax translocation to the mitochondria. (**A**) Schematic representation of the structure of the MKK7–JNK fusion proteins (WT or KN), which comprise mouse MKK7α1 linked to rat JNK1β1 by the Flag epitope sequence. The kinase-negative mutant of JNK1 was generated by replacement of Lys^{434} and Lys^{435} with methionines. (**B**) COS-1 cells were transfected for 13 h with expression vectors for GFP–Bax, the mitochondrial marker DsRed-Mito and the caspase inhibitor p35, together with a vector for MKK7–JNK (WT or KN) or the corresponding empty vector, as indicated. They were then examined for the distribution of GFP–Bax (green) and mitochondria (red) by fluorescence microscopy; the two separate images for each representative cell are also shown superimposed (overlay). (**C**) COS-1 cells were transfected for the indicated times as in (B), and the percentage of cells exhibiting GFP–Bax localization to mitochondria was determined. Data are means ± s.d. of values obtained from five fields of 30–150 cells in each of three independent experiments. (**D**) COS-1 cells were transfected for 20 h with expression vectors for GFP and MKK7–JNK(WT or KN) in the absence or presence of a vector for p35, as indicated. The transfection efficiency was ~75%, as determined by monitoring the expression of GFP. The cells were then subjected to subcellular fractionation, and the amount of endogenous Bax and that of cytochrome *c* in the mitochondrial and cytosolic fraction were assessed by immunoblot analysis (IB) with antibodies specific for these proteins. The amounts of the mitochondrial marker F_0F_1-ATPase and cytosolic marker α-tubulin were similarly assessed as an internal standard.

Activation of c-Jun-dependent transcription was blocked by coexpression of a DN form of c-Jun (Figure 3A). However, expression of DN c-Jun did not inhibit the translocation of GFP–Bax to mitochondria induced by MKK7–JNK(WT) (Figure 3B). The MKK7–JNK(WT)-induced increase in the amount of endogenous Bax in the mitochondrial fraction was also unaffected by DN c-Jun (Supplementary Figure 5). These results therefore suggest that JNK induces Bax translocation to mitochondria independently of the transcriptional activity of c-Jun.

Since previous reports have shown that Bax translocation to the mitochondria in response to apoptotic stimuli is suppressed by the PI3K–Akt pathway (Yamaguchi and Wang, 2001; Tsuruta *et al*, 2002; Molton *et al*, 2003), we examined the involvement of the PI3K–Akt pathway in JNK-mediated Bax translocation. We found that expression of MKK7–JNK(WT) or of MKK7–JNK(KN) had no effect on the EGF-induced activation and phosphorylation of Akt at Ser-473 in COS-1 cells (Supplementary Figure 6). Moreover, expression of constitutively active or DN Akt constructs did not affect the level of JNK phosphorylation (Tsuruta *et al*, 2002) or the JNK-induced GFP–Bax translocation to the mitochondria (Supplementary Figure 7). These results suggest that JNK does not induce Bax translocation by inhibiting the PI3K–Akt pathway.

The Bcl-2 family member Bim can regulate Bax translocation and has been reported to be a target of JNK (Lei and Davis, 2003; Putcha *et al*, 2003). We therefore examined whether Bim is phosphorylated by JNK under the conditions used in this study and whether Bim phosphorylation correlates with Bax translocation to mitochondria. Bim phosphorylation was monitored by a shift in its electrophoretical mobility on SDS–PAGE as described (Lei and Davis, 2003; Putcha *et al*, 2003). Immunoblot analysis showed a mobility shift of Bim in response to anisomycin treatment. The JNK inhibitor SP600125, however, had little effect on the anisomycin-induced mobility shift of Bim, whereas it effectively blocked phosphorylation of c-Jun (Supplementary Figure 8). Importantly, expression of MKK7–JNK(WT) promoted Bax translocation to mitochondria, but did not induce the mobility shift of Bim (Supplementary Figure 8). These data suggest that a kinase or kinases other than JNK are activated by

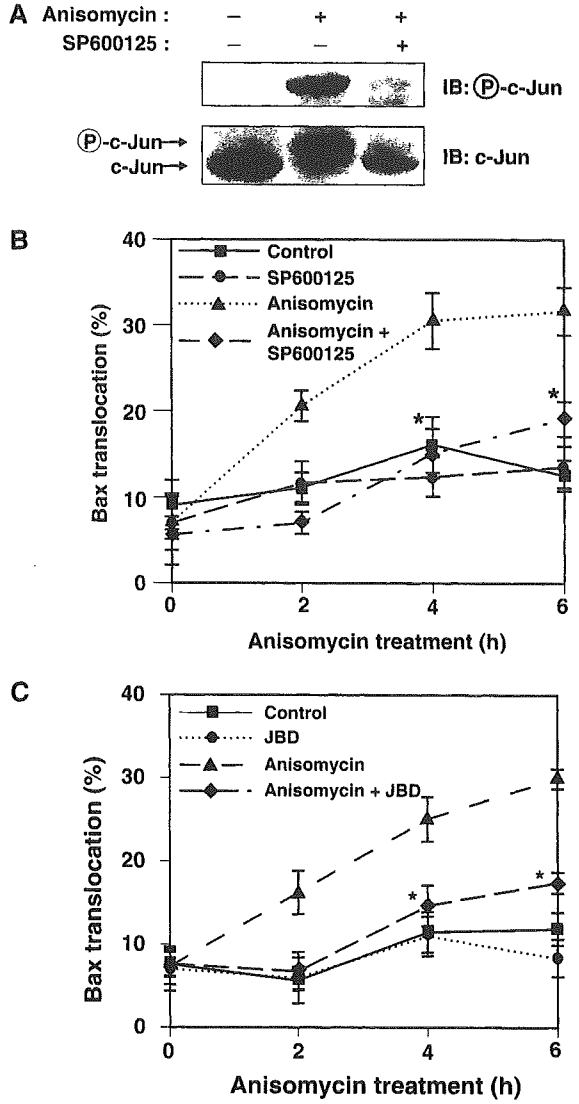

Figure 2 JNK is required for stress-induced translocation of Bax to the mitochondria. (**A**) COS-1 cells were incubated first for 30 min with or without 20 μM SP600125 and then for 1 h in the presence or absence of anisomycin (10 μg/ml). Cell lysates were then subjected to immunoblot analysis with antibodies to phosphorylated c-Jun or to c-Jun. The anisomycin-induced shift in the electrophoretic mobility of the band detected by the antibody to c-Jun reflects phosphorylation of c-Jun. (**B**) COS-1 cells were transfected for 11 h with expression vectors for GFP–Bax and p35, were pretreated with or without 20 μM SP600125 for 30 min, and were then incubated for the indicated times in the presence or absence of anisomycin (10 μg/ml). The percentage of cells in which GFP–Bax was localized to mitochondria was then determined. Data are means ± s.d. of values obtained from five fields of 30–150 cells in each of three independent experiments (*$P<0.0005$ as compared with the anisomycin group). (**C**) COS-1 cells were transfected for 11 h with expression vectors for GFP–Bax and p35, together with a vector for JBD or the corresponding empty vector, as indicated. The cells were then incubated for the indicated times in the presence or absence of 10 μg/ml anisomycin, after which the percentage of cells exhibiting GFP–Bax localization to mitochondria was determined. Data are means ± s.d. of values obtained from five fields of 30–150 cells in each of two independent experiments (*$P<0.0005$ as compared with the anisomycin group).

anisomycin and phosphorylate Bim, and that JNK induces Bax translocation independently of Bim phosphorylation at least in this system.

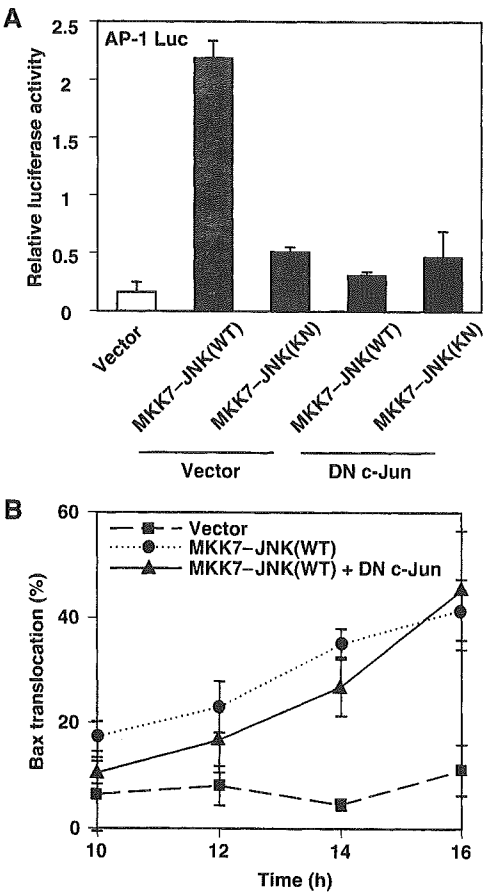

Figure 3 JNK induces Bax translocation to the mitochondria independently of c-Jun. (**A**) COS-1 cells were transfected for 1 day with an AP-1-luciferase reporter plasmid and expression vectors for MKK7–JNK(WT or KN) and a DN form of c-Jun or the corresponding empty vectors, as indicated. The normalized luciferase activity of cell lysates was then determined. Data represent the means ± s.d. of triplicate determinations from three independent experiments. (**B**) COS-1 cells were transfected for the indicated times with expression vectors for GFP–Bax and p35 together with vectors for MKK7–JNK(WT or KN) and DN c-Jun, as indicated. The percentage of cells exhibiting GFP–Bax localization to mitochondria was then determined. Data are means ± s.d. of values obtained from five fields of 30–150 cells in each of two independent experiments.

JNK phosphorylates 14-3-3ζ at Ser-184 and 14-3-3σ at Ser-186 in vitro

Under resting conditions, 14-3-3 proteins function as cytoplasmic anchors of Bax and prevent Bax from translocating to the mitochondria (Nomura *et al*, 2003). Consistent with this observation, targeted disruption of the 14-3-3σ gene was shown to accelerate Bax translocation to the mitochondria in human HCT116 cells (Samuel *et al*, 2001). These findings prompted us to investigate the possibility that JNK promotes Bax translocation to mitochondria by regulating the interaction between Bax and 14-3-3 proteins. Previous reports have shown that several isoforms of 14-3-3 are phosphorylated *in vivo* at a serine residue in the region between α-helices 7 and 8 (Ser-186 of 14-3-3β and Ser-184 of 14-3-3ζ), although the kinase or kinases responsible for this phosphorylation were not identified (Aitken *et al*, 1995). Interestingly, this residue conforms to the consensus sequence for JNK phosphorylation (Ser-Pro), and resides within the putative Bax-binding region (Figure 4A) (Nomura *et al*, 2003). We thus

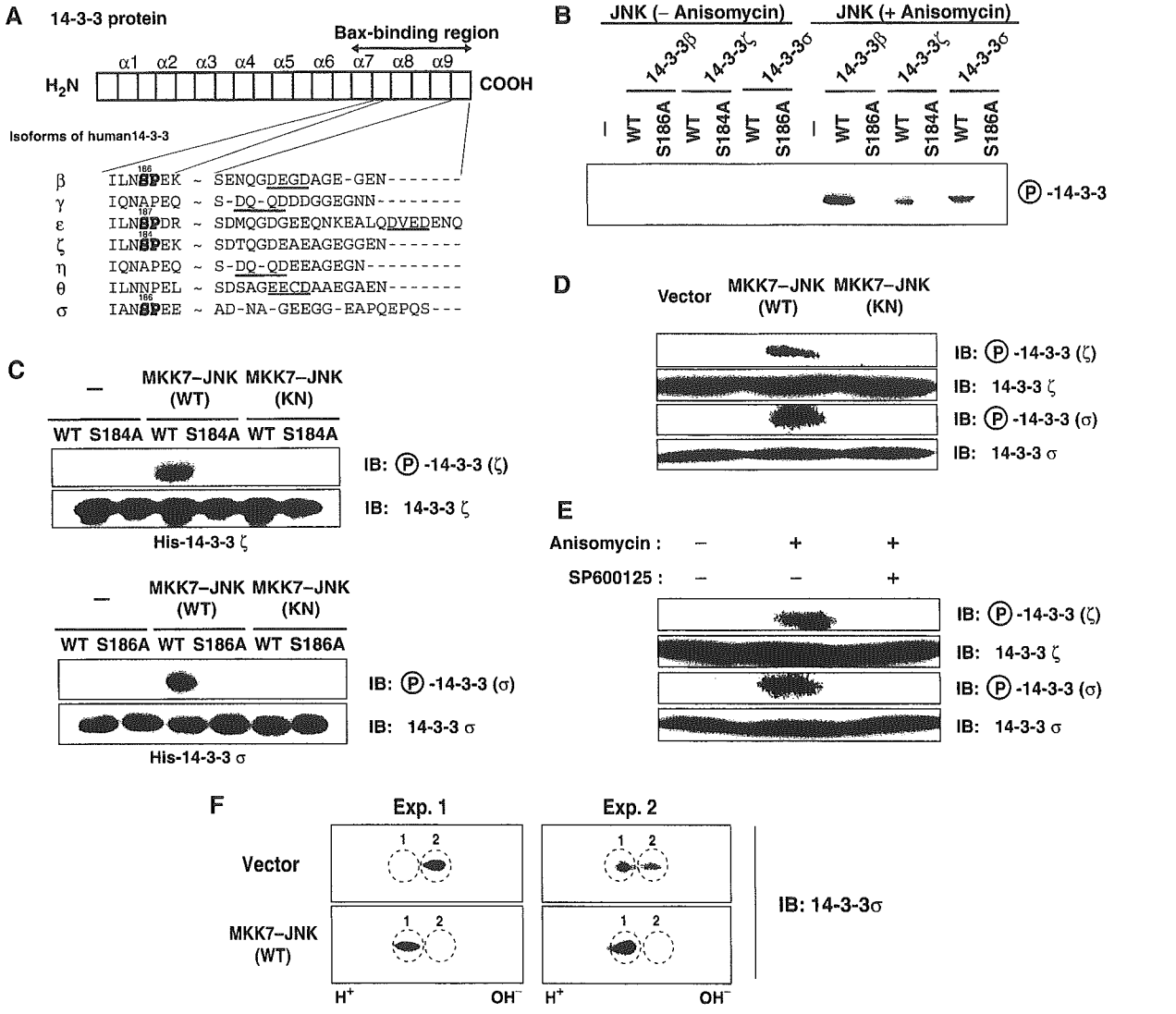

Figure 4 JNK phosphorylates 14-3-3ζ and 14-3-3σ both *in vitro* and *in vivo*. (**A**) Schematic representation of the structure of human 14-3-3 proteins and the amino-acid sequences surrounding putative JNK phosphorylation sites (SP, shown in bold) and caspase-3 cleavage sites ((D/E)XXD, underlined) in the Bax-binding region of the indicated isoforms. The numbers indicate the position of putative phosphorylation sites. (**B**) COS-1 cells were transfected for 24 h with an expression vector for Flag-tagged JNK and then incubated for 1 h in the absence or presence of anisomycin (10 μg/ml). Flag–JNK was immunoprecipitated from cell lysates with antibodies to Flag and incubated with the indicated recombinant His_6-tagged 14-3-3 proteins (WT or Ser→Ala mutants) in the presence of [γ-^{32}P]ATP. The amount of JNK immunoprecipitated from anisomycin-treated cell extracts was comparable to that from untreated cell extracts under the conditions used in this *in vitro* kinase assay (data not shown). Phosphorylation of 14-3-3 proteins was detected by electrophoresis and autoradiography. (**C**) Recombinant His_6-tagged 14-3-3 proteins (WT or mutant) were incubated with or without recombinant MKK7–JNK(WT or KN) in the presence of ATP and were then subjected to immunoblot analysis with antibodies specific for 14-3-3ζ or 14-3-3ζ phosphorylated on Ser^{184} (upper panels) or for 14-3-3σ or 14-3-3σ phosphorylated on Ser^{186} (lower panels). (**D**) HCT116 cells were transfected for 1 day with an expression vector for MKK7–JNK(WT or KN) or the corresponding empty vector, after which cell lysates were subjected to immunoblot analysis with the antibodies described in (C). (**E**) HCT116 cells were incubated first for 30 min with or without 20 μM SP600125 and then for 3 h in the presence or absence of anisomycin (10 μg/ml). Cell lysates were then subjected to immunoblot analysis as described in (D). (**F**) HCT116 cells were transfected for 1 day with an expression vector for MKK7–JNK(WT) or the corresponding empty vector, after which cell lysates were subjected to two-dimensional gel electrophoresis and immunoblot analysis with anti-14-3-3σ antibody. Two typical results (Exp. 1 and Exp. 2) are shown. The ratio between Spot 1 and Spot 2 in control cells varied among experiments, but expression of MKK7–JNK (WT) repeatedly increased Spot 1 and abolished Spot 2.

first examined whether JNK is capable of phosphorylating 14-3-3 proteins. Active JNK immunoprecipitated from anisomycin-treated COS-1 cell extracts efficiently phosphorylated recombinant His-tagged 14-3-3β, 14-3-3ζ and 14-3-3σ in an *in vitro* kinase assay (Figure 4B). JNK immunoprecipitates prepared from untreated cells did not phosphorylate recombinant 14-3-3 proteins, confirming that the kinase activity of JNK was responsible for this phosphorylation. Mutant proteins in which Ser-184 of 14-3-3ζ or Ser-186 of 14-3-3β or 14-3-3σ was replaced with alanine were not phosphorylated by the active JNK immunoprecipitated from anisomycin-treated cells (Figure 4B), indicating that these serine residues are the JNK-mediated phosphorylation sites *in vitro*.

To further indicate that Ser-184 of 14-3-3ζ and Ser-186 of 14-3-3σ are phosphorylated by JNK, we prepared antibodies to phosphopeptides corresponding to these phosphorylation

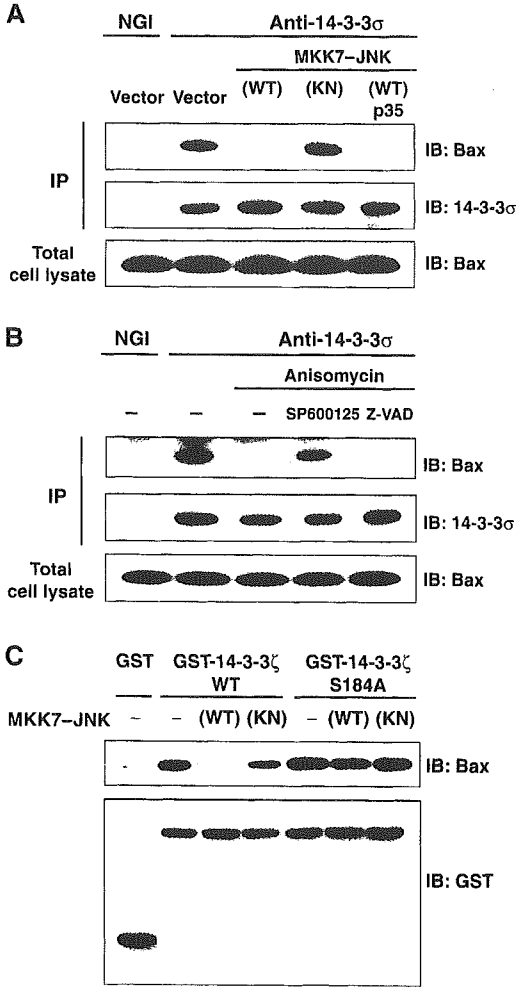

Figure 5 JNK promotes dissociation of Bax from 14-3-3 proteins. (**A**) HCT116 cells were transfected for 24 h with expression vectors for GFP, MKK7–JNK(WT or KN) and p35, as indicated. Cell lysates were then subjected either to immunoblot analysis with antibodies to Bax or to immunoprecipitation (IP) with antibodies to 14-3-3σ (or to normal goat IgG (NGI) precipitation); the resulting precipitates were subjected to immunoblot analysis with antibodies to 14-3-3σ and to Bax. (**B**) HCT116 cells were incubated first for 30 min with or without 20 μM SP600125 or 100 μM Z-VAD-CH_2DCB and then for 3 h in the presence or absence of anisomycin (10 μg/ml). Cell lysates were then subjected to immunoprecipitation and immunoblot analysis as described in (A). (**C**) Equal amounts of recombinant GST-14-3-3ζ (WT or Ser^{184}→Ala mutant) or GST alone were incubated with or without recombinant MKK7–JNK(WT or KN) in the presence of ATP for 30 min, and the GST proteins were precipitated with glutathione-sepharose beads. The beads were then incubated with HeLa cell lysates, and subjected to immunoblot analysis with antibodies to Bax or to GST.

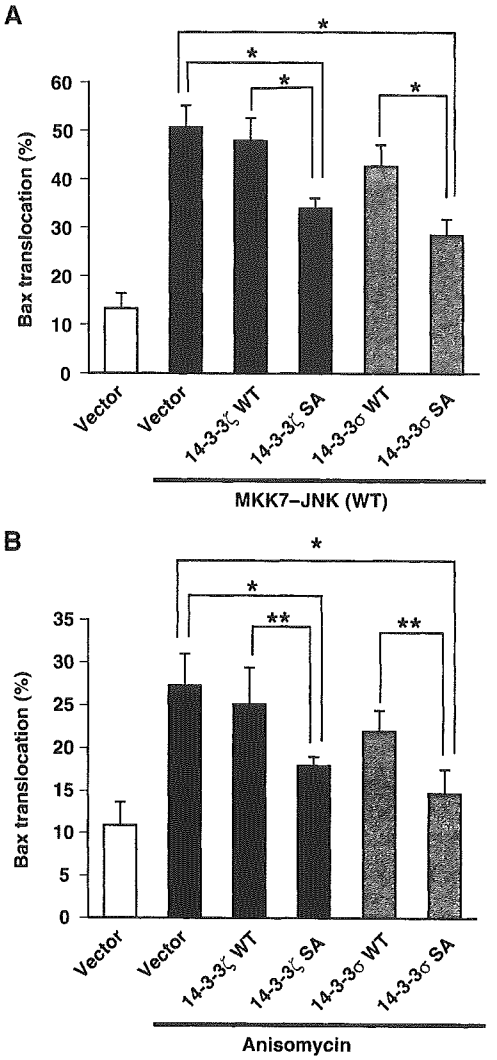

Figure 6 14-3-3 mutants inhibit JNK-induced Bax translocation to mitochondria. (**A**) COS-1 cells were transfected for 16 h with expression vectors for GFP–Bax and p35 together with those for MKK7–JNK(WT) and either 14-3-3ζ or 14-3-3σ. The percentage of cells exhibiting GFP–Bax localization to the mitochondria was then determined. Data are means ± s.d. of values obtained from five fields of 30–150 cells in each of three independent experiments (*$P<0.0005$). (**B**) COS-1 cells were transfected for 11.5 h with expression vectors for GFP–Bax, p35 and either 14-3-3ζ or 14-3-3σ, and were incubated for 6 h in the presence or absence of anisomycin (10 μg/ml). The percentage of cells in which GFP–Bax was localized to the mitochondria was then determined and shown as in (A) (*$P<0.0005$ and **$P<0.005$).

sites. The anti-phospho-Ser^{184}-14-3-3ζ and anti-phospho-Ser^{186}-14-3-3σ antibodies recognized recombinant 14-3-3 proteins (14-3-3ζ and σ) that had been phosphorylated by recombinant MKK7–JNK(WT), but not those incubated with MKK7–JNK(KN) (Figure 4C). Moreover, these antibodies did not react with the Ser→Ala (SA) mutants of the corresponding 14-3-3 proteins, confirming that they specifically recognize phosphorylated 14-3-3 proteins at these serine residues.

JNK phosphorylates 14-3-3ζ at Ser-184 and 14-3-3σ at Ser-186 in vivo

To determine whether JNK also phosphorylates 14-3-3 *in vivo*, we examined the phosphorylation status of 14-3-3 proteins with the anti-phospho-14-3-3 antibodies. We used HCT116 cells in which ζ and σ isoforms of 14-3-3 are expressed endogenously. Expression of MKK7–JNK(WT), but not MKK7–JNK(KN), in HCT116 cells increased the bands reactive to the antibodies raised against phosphopeptides for 14-3-3ζ at Ser-184 and 14-3-3σ at Ser-186 (Figure 4D), suggesting that endogenous 14-3-3 proteins became phosphorylated upon JNK activation. We then addressed whether the phosphorylation of 14-3-3 is induced by cellular stresses. Exposure of HCT116 cells to anisomycin induced the phosphorylation of 14-3-3 proteins, revealed by the antibodies for 14-3-3ζ at Ser-184 and 14-3-3σ at Ser-186 (Figure 4E). The concentration of anisomycin required for phosphorylation of 14-3-3 was similar to that required for

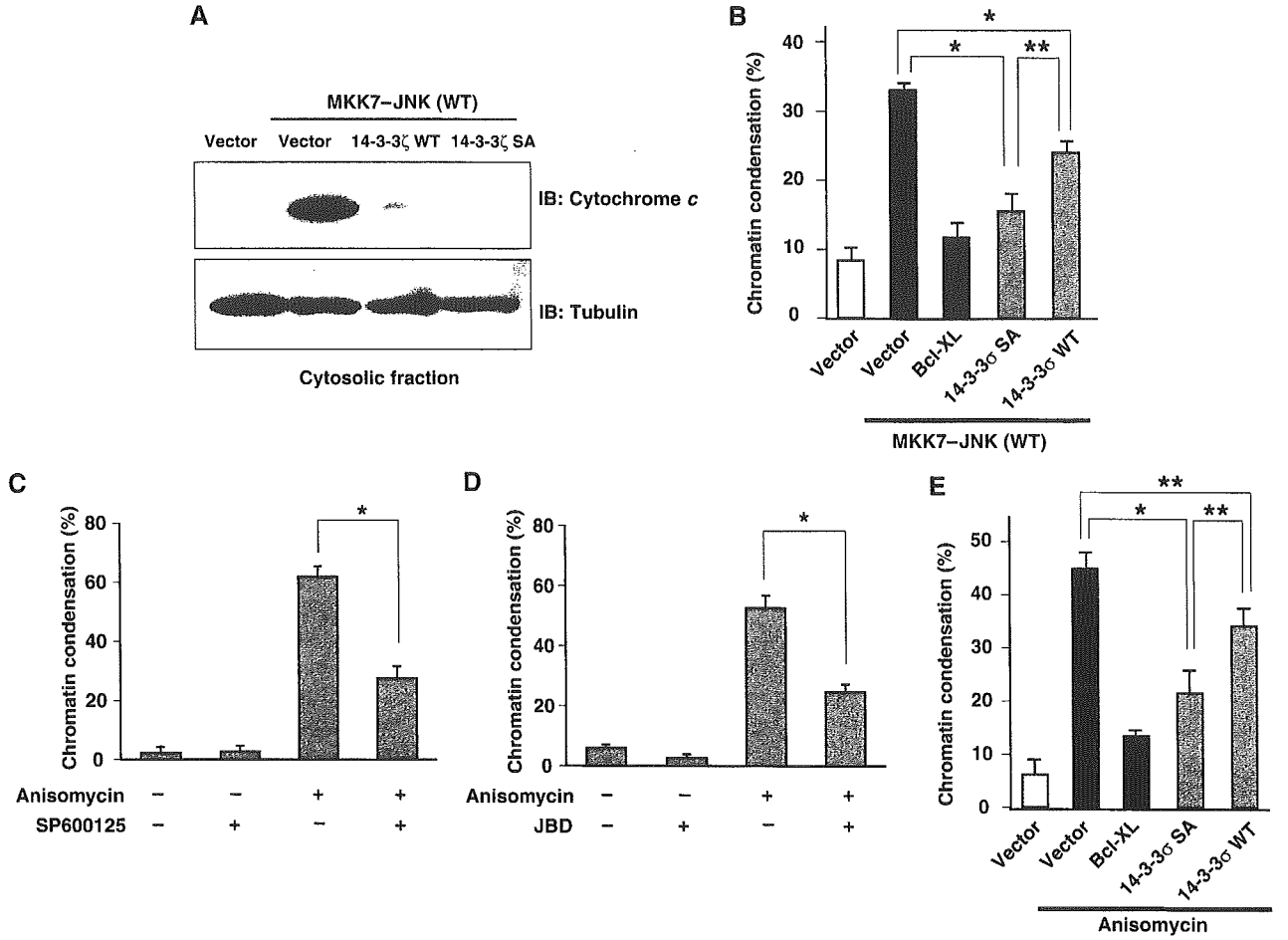

Figure 7 14-3-3 mutants inhibit JNK-induced cell death. (**A**) COS-1 cells were transfected for 20 h with expression vectors for GFP, MKK7–JNK(WT), and either 14-3-3ζ WT or 14-3-3ζ S184A, as indicated, and were then subjected to subcellular fractionation. The amounts of endogenous cytochrome *c* and α-tubulin (internal control) in the cytosolic fraction were determined by immunoblot analysis with specific antibodies. (**B**) COS-1 cells were transfected for 20 h with expression vectors for GFP, MKK7–JNK(WT) and either Bcl-XL, 14-3-3σ S186A or the corresponding WT proteins, as indicated. They were then stained with Hoechst 33342 (6.7 μg/ml) for 10 min, and the percentage of GFP-positive cells with pyknotic nuclei was determined. Data are means ± s.d. of values obtained from three fields of 200–300 cells in each of three independent experiments (*$P<0.0005$ and **$P<0.005$). (**C**) HeLa cells were incubated first for 30 min with or without 20 μM SP600125 and then for 3 h in the presence or absence of anisomycin (10 μg/ml). They were then stained with Hoechst 33342 (6.7 μg/ml) for 10 min, and the percentage of cells with pyknotic nuclei was determined. Data are means ± s.d. of values obtained from three fields of 100–200 cells in each of two independent experiments (*$P<0.0005$). (**D**) HeLa cells were transfected with expression vectors for GFP and JBD and then for 3 h in the presence or absence of anisomycin (10 μg/ml). They were then stained with Hoechst 33342 (6.7 μg/ml) for 10 min, and the percentage of GFP-positive cells with pyknotic nuclei was determined. Data are means ± s.d. of values obtained from three fields of 100–150 cells (*$P<0.0005$). (**E**) HeLa cells were transfected with expression vectors for GFP and either Bcl-XL, 14-3-3σ S186A or the corresponding WT protein, and then for 3 h in the presence or absence of anisomycin (10 μg/ml). They were then stained with Hoechst 33342 (6.7 μg/ml) for 10 min, and the percentage of GFP-positive cells with pyknotic nuclei was determined and shown as in (C) (*$P<0.0005$ and **$P<0.005$).

JNK activation (data not shown). Furthermore, anisomycin-induced phosphorylation of 14-3-3 proteins (14-3-3ζ and 14-3-3σ) was inhibited by pretreatment of cells with the JNK inhibitor SP600125 (Figure 4E), suggesting that JNK activation is required for anisomycin-induced 14-3-3 phosphorylation *in vivo*.

To further examine phosphorylation of 14-3-3 upon JNK activation *in vivo*, we carried out two-dimensional gel electrophoresis to separate hyper- and hypophosphorylated forms of 14-3-3. We detected two spots of 14-3-3σ in control (vector-transfected) HCT116 cells. Expression of MKK7–JNK(WT) (Figure 4F) or treatment with anisomycin (data not shown) resulted in a marked increase in the spot with greater negative charge (Spot 1) and a corresponding decrease in the other spot (Spot 2). We confirmed that Spot 1 is a phosphorylated form of Spot 2, as alkaline phosphatase treatment of MKK7–JNK(WT)-expressing cell extracts reduced Spot 1 and increased Spot 2 (data not shown). These results suggest that a high proportion of 14-3-3σ becomes phosphorylated upon JNK activation.

JNK promotes dissociation of Bax from 14-3-3 proteins

We next asked whether JNK-mediated phosphorylation of 14-3-3 affects the interaction between Bax and 14-3-3. Immunoprecipitation of 14-3-3σ from HCT116 cell lysates resulted in the co-precipitation of endogenous Bax (Figure 5A). Expression of MKK7–JNK(WT), but not that of MKK7–JNK(KN), resulted in a marked decrease in the amount of Bax that co-precipitated with 14-3-3σ. This effect of MKK7–JNK(WT) was not affected by coexpression of p35,

suggesting that JNK promotes the dissociation of Bax from 14-3-3 independently of caspase activation.

Exposure of HCT116 cells to anisomycin also reduced the amount of Bax that co-immunoprecipitated with 14-3-3σ (Figure 5B). Pretreatment of cells with the caspase inhibitor Z-VAD-CH_2DCB had no effect on the anisomycin-induced dissociation of Bax from 14-3-3, whereas pretreatment with the JNK inhibitor SP600125 blocked this effect of anisomycin. These results thus suggest that JNK mediates the anisomycin-induced dissociation of Bax from 14-3-3.

To examine further whether JNK-induced dissociation of Bax from 14-3-3 is dependent on the phosphorylation status of 14-3-3, we performed glutathione *S*-transferase (GST) pull-down assays with a GST–14-3-3ζ fusion protein (Figure 5C). Incubation of GST–14-3-3ζ, but not that of GST alone, with HeLa cell lysates resulted in the co-precipitation of Bax by glutathione-Sepharose. However, prior phosphorylation of GST-14-3-3ζ by MKK7–JNK(WT) led to a marked decrease (approximately 90% reduction) in the amount of Bax that co-precipitated with GST-14-3-3ζ. The S184A mutant of GST-14-3-3ζ precipitated similar amounts of Bax, regardless of whether or not it had been preincubated with MKK7–JNK(WT). These results are thus consistent with the notion that JNK-mediated phosphorylation of 14-3-3ζ at Ser184 reduces its affinity for Bax.

14-3-3 mutants inhibit Bax translocation, cytochrome c release and cell death

If 14-3-3 is a major target for JNK in induction of Bax translocation, one might expect that expression of a phosphorylation site mutant of 14-3-3 would block JNK-induced Bax translocation. Indeed, expression of either 14-3-3ζ S184A or 14-3-3σ S186A mutant inhibited MKK7–JNK- and anisomycin-induced GFP–Bax translocation to mitochondria (Figure 6A and B and Supplementary Figure 9). In addition, when distribution of endogenous Bax was assessed by subcellular fractionation, expression of 14-3-3ζ S184A mutant inhibited the increase of Bax protein in the mitochondrial fraction induced by MKK7–JNK (Supplementary Figure 10). Importantly, in both assays, 14-3-3 WT was less effective than its SA mutant in suppression of JNK-induced Bax translocation (Figure 6A and B and Supplementary Figure 10), suggesting strongly that phosphorylation of 14-3-3 at this Ser residue is critical for Bax translocation to mitochondria upon JNK activation.

We next examined whether 14-3-3 mutants inhibited JNK-induced cytochrome *c* release and cell death. The amount of endogenous cytochrome *c* detected in the cytosolic fraction was increased when MKK7–JNK(WT), but not MKK7–JNK(KN), was expressed in COS-1 cells (Figure 7A and data not shown). In contrast, co-expression of 14-3-3ζ S184A mutant, and that of the corresponding 14-3-3 WT to a lesser extent, inhibited MKK7–JNK (WT)-induced cytochrome *c* release, whereas the amount of the cytosolic marker α-tubulin in the cytosolic fraction was unaffected by MKK7–JNK or the 14-3-3 mutants (Figure 7A). Expression of MKK7–JNK (WT) in COS-1 cells induced chromatin condensation, an indication of cell death (Figure 7B). However, expression of 14-3-3σ SA mutant rendered the cells resistant to this effect of MKK7–JNK (WT) (Figure 7B). Moreover, 14-3-3σ WT was less effective in protecting cells from MKK7–JNK (WT)-induced cell death, compared to the 14-3-3σ SA mutant (Figure 7B). We next asked whether the 14-3-3σ mutant can inhibit anisomycin-induced cell death. Treatment of HeLa cells with anisomycin resulted in cell death, and pretreatment with SP600125 or coexpression of JBD or DN JNK partially blocked this effect (Figure 7C and D and Supplementary Figure 11), suggesting that JNK is required for anisomycin-induced cell death in HeLa cells. We found that expression of 14-3-3σ SA mutant blocked anisomycin-induced cell death, and 14-3-3σ WT was less effective compared to the 14-3-3σ SA mutant (Figure 7E), supporting the notion that phosphorylation of 14-3-3 by JNK plays an important role in JNK-mediated cell death.

Discussion

Recent studies have demonstrated that JNK plays a pivotal role in activation of the intrinsic apoptotic pathway that is mediated by mitochondria in response to cellular stress (Davis, 2000). Although Bax has been shown to be necessary for this action of JNK, the nature of the functional relation between these two proteins has been unclear. We now provide several lines of evidence that demonstrate that JNK-mediated phosphorylation of 14-3-3 induces the release of Bax from 14-3-3 and triggers its translocation to the mitochondria: (1) expression of an active form of JNK promoted Bax translocation to mitochondria; (2) inhibition of JNK (either by a chemical inhibitor or by a DN mutant) reduced the extent of Bax translocation to mitochondria in response to cellular stress; (3) JNK phosphorylated 14-3-3ζ at Ser-184 and 14-3-3σ at Ser-186 both *in vitro* and *in vivo*, and such phosphorylation reduced the affinity of 14-3-3 proteins for Bax; (4) expression of active JNK or treatment of cells with anisomycin induced the dissociation of Bax from 14-3-3 proteins; and (5) expression of phosphorylation site mutants of 14-3-3 proteins inhibited Bax translocation to mitochondria. These results strongly indicate that JNK regulates the activity of Bax by phosphorylating 14-3-3 proteins.

The initial studies of the role of JNK in apoptotic signals were performed by investigating neuronal cell death in response to neurotrophic factor withdrawal (Xia *et al*, 1995). The role for JNK in stress-induced neuronal cell death was confirmed by the studies of mice with a targeted disruption of the neuronal gene JNK3 (Yang *et al*, 1997). Although the JNK3 knockout mice are developmentally normal, they are resistant to excitotoxins. A similar resistance was observed in mice with a germ-line mutation in the c-Jun gene that replaced the JNK phosphorylation sites with alanine (Behrens *et al*, 1999). These data suggested that JNK mediates transcription-dependent apoptotic signals in neurons. In contrast, in non-neuronal cells, the JNK-mediated cytochrome *c* release and apoptosis induced by UV do not require *de novo* gene expression (Tournier *et al*, 2000). It is thus likely that relevant targets of JNK required for cytochrome *c* release and apoptosis are already present in these cells. Potential targets of JNK that may regulate cytochrome *c* release and apoptosis include members of the Bcl-2 family. The anti-apoptotic members Bcl-2, Bcl-x_L and Mcl-1, and the pro-apoptotic members Bad, Bim and Bmf are phosphorylated by JNK, although the significance of these phosphorylation events remains unclear (Ito *et al*, 1997; Maundrell *et al*, 1997; Kharbanda *et al*, 2000; Donovan *et al*, 2002; Inoshita *et al*, 2002; Lei and Davis, 2003; Putcha *et al*, 2003). We have

now shown that expression of phosphorylation site mutants of 14-3-3, and 14-3-3 WT to a lesser extent, suppressed JNK-induced Bax translocation, mitochondrial cytochrome *c* release and subsequent cell death. We confirmed that the 14-3-3 mutant did not hamper JNK-mediated phosphorylation of other targets such as c-Jun (F Tsuruta and Y Gotoh, unpublished results). These results strongly suggest that 14-3-3 protein is a major target of JNK in induction of these apoptotic events.

The JNK-mediated phosphorylation of 14-3-3β and 14-3-3ζ was found to occur at the previously identified phosphorylation sites (Aitken *et al*, 1995); 14-3-3β and 14-3-3ζ phosphorylated at these sites were named 14-3-3α and 14-3-3δ, respectively. It remains to be determined how such phosphorylation leads to the dissociation of Bax from 14-3-3. However, since the JNK phosphorylation sites reside within the domain responsible for the interaction of 14-3-3 with Bax (Nomura *et al*, 2003), it is likely that phosphorylation impairs the interaction at the binding interface. Alternatively, although the overall structure of 14-3-3 proteins is thought to be relatively rigid (Liu *et al*, 1995; Xiao *et al*, 1995), it is possible that phosphorylation might change the global conformation of 14-3-3 and thereby induce the dissociation of Bax.

On the Bax side, the 14-3-3-interacting domains are in the NH_2- and COOH-terminal regions (Nomura *et al*, 2003). Interestingly, previous studies have proposed that these regions are masked when Bax is in the inactive form and are exposed upon activation. Indeed, antibodies against certain epitopes at the NH_2-terminal region (cf. 6A7 monoclonal antibody) can react only with active Bax (Nechushtan *et al*, 1999; Lei *et al*, 2002). It is thus possible that 14-3-3 proteins physically conceal the NH_2- and COOH-terminal domains of Bax and thereby maintain it in its inactive form, and that dissociation of Bax from 14-3-3 may be essential for its activation in addition to the conformational change of Bax. According to this scenario, our observation that phosphorylation of 14-3-3 by JNK releases Bax from 14-3-3 may explain how JNK activates Bax. Consistent with this notion, targeted disruption of JNK genes has been shown to prevent the activation of Bax in response to cellular stresses, as judged by the lack of reactivity toward the 6A7 antibody (Lei *et al*, 2002).

Another proposed mechanism of Bax activation is a conformational change due to acidification or alkalization of the cytoplasmic pH (Khaled *et al*, 1999; Nomura *et al*, 2003). However, we could not detect a significant change in the signal level of a pH indicator incorporated into the cytoplasm in the presence or absence of activated JNK in our preliminary experiments (F Tsuruta and Y Gotoh, unpublished results), suggesting that it is unlikely that JNK promotes Bax activation indirectly through regulation of cytoplasmic pH.

Whereas we have shown that three 14-3-3 isoforms (β, ζ and σ) serve as JNK targets, some isoforms (γ, η and θ) do not possess a corresponding JNK phosphorylation site. One of these isoforms (θ) has been reported to be cleaved by caspase, resulting in dissociation of Bax (Nomura *et al*, 2003). Our results indicate that caspase activity is dispensable for the JNK-dependent dissociation of Bax from 14-3-3, indicating the existence of two independent mechanisms to regulate their dissociation. Since caspase is activated downstream of JNK, it is possible that phosphorylation-dependent release of Bax from 14-3-3 takes place first, and the caspase-dependent release of Bax subsequently amplifies the apoptotic signal through positive feedback.

Recently, it has been reported that Ku70 and Humanin also prevent apoptosis through sequestration of Bax (Guo *et al*, 2003; Sawada *et al*, 2003). However, Sawada *et al* (2003) have shown that the absence of Ku70 is not sufficient for inducing the apoptotic level of Bax translocation to mitochondria in the absence of apoptotic stimuli. Guo *et al* (2003) have also demonstrated that elimination of endogenous Humanin does not induce Bax translocation to mitochondria and apoptosis in healthy cells. It is thus likely that several cytoplasmic anchors for Bax work in parallel to sequester Bax from mitochondria, and dissociation of Bax from all or some of these cytoplasmic anchors may be required for initiation of Bax translocation to mitochondria.

In conclusion, we have demonstrated that JNK promotes Bax translocation to mitochondria through phosphorylation of 14-3-3 proteins. This finding may account at least in part for the apoptosis-inducing activity of the JNK and shed light on the mechanism of stress-induced apoptosis.

Materials and methods

The Materials and methods used in this study are described in Supplementary data.

Supplementary data

Supplementary data are available at *The EMBO Journal* Online.

Acknowledgements

We thank J Inagawa and K Ueda for technical supports with the two-dimensional gel electrophoresis, Drs R Dolmetsch and X Wang for critical reading of the manuscript, Drs M Miura, M Yaffe, H Fu, B Vogelstein and R Davis for providing reagents, and members of the Gotoh laboratory for helpful discussions and technical support.

References

Aitken A, Howell S, Jones D, Madrazo J, Patel Y (1995) 14-3-3 alpha and delta are the phosphorylated forms of raf-activating 14-3-3 beta and zeta. *In vivo* stoichiometric phosphorylation in brain at a Ser-Pro-Glu-Lys MOTIF. *J Biol Chem* **270:** 5706–5709

Behrens A, Sibilia M, Wagner EF (1999) Amino-terminal phosphorylation of c-Jun regulates stress-induced apoptosis and cellular proliferation. *Nat Genet* **21:** 326–329

Benton R, Palacios IM, Johnston DS (2002) Drosophila 14-3-3/PAR-5 is an essential mediator of PAR-1 function in axis formation. *Dev Cell* **3:** 659–671

Brunet A, Bonni A, Zigmond MJ, Lin MZ, Juo P, Hu LS, Anderson MJ, Arden KC, Blenis J, Greenberg ME (1999) Akt promotes cell survival by phosphorylating and inhibiting a Forkhead transcription factor. *Cell* **96:** 857–868

Datta SR, Dudek H, Tao X, Masters S, Fu H, Gotoh Y, Greenberg ME (1997) Akt phosphorylation of BAD couples survival signals to the cell-intrinsic death machinery. *Cell* **91:** 231–241

Davis RJ (2000) Signal transduction by the JNK group of MAP kinases. *Cell* **103:** 239–252

Dickens M, Rogers JS, Cavanagh J, Raitano A, Xia Z, Halpern JR, Greenberg ME, Sawyers CL, Davis RJ (1997) A cytoplasmic inhibitor of the JNK signal transduction pathway. *Science* **277:** 693–696

Donovan N, Becker EB, Konishi Y, Bonni A (2002) JNK phosphorylation and activation of BAD couples the stress-activated

signaling pathway to the cell death machinery. *J Biol Chem* **277:** 40944–40949

Du X, Fox JE, Pei S (1996) Identification of a binding sequence for the 14-3-3 protein within the cytoplasmic domain of the adhesion receptor, platelet glycoprotein Ib alpha. *J Biol Chem* **271:** 7362–7367

Gilmore AP, Metcalfe AD, Romer LH, Streuli CH (2000) Integrin-mediated survival signals regulate the apoptotic function of Bax through its conformation and subcellular localization. *J Cell Biol* **149:** 431–446

Gross A, McDonnell JM, Korsmeyer SJ (1999) BCL-2 family members and the mitochondria in apoptosis. *Genes Dev* **13:** 1899–1911

Guo B, Zhai D, Cabezas E, Welsh K, Nouraini S, Satterthwait AC, Reed JC (2003) Humanin peptide suppresses apoptosis by interfering with Bax activation. *Nature* **423:** 456–461

Harris CA, Johnson Jr EM (2001) BH3-only Bcl-2 family members are coordinately regulated by the JNK pathway and require Bax to induce apoptosis in neurons. *J Biol Chem* **276:** 37754–37760

Hsu YT, Wolter KG, Youle RJ (1997) Cytosol-to-membrane redistribution of Bax and Bcl-X(L) during apoptosis. *Proc Natl Acad Sci USA* **94:** 3668–3672

Inoshita S, Takeda K, Hatai T, Terada Y, Sano M, Hata J, Umezawa A, Ichijo H (2002) Phosphorylation and inactivation of myeloid cell leukemia 1 by JNK in response to oxidative stress. *J Biol Chem* **277:** 43730–43734

Ito T, Deng X, Carr B, May WS (1997) Bcl-2 phosphorylation required for anti-apoptosis function. *J Biol Chem* **272:** 11671–11673

Khaled AR, Kim K, Hofmeister R, Muegge K, Durum SK (1999) Withdrawal of IL-7 induces Bax translocation from cytosol to mitochondria through a rise in intracellular pH. *Proc Natl Acad Sci USA* **96:** 14476–14481

Kharbanda S, Saxena S, Yoshida K, Pandey P, Kaneki M, Wang Q, Cheng K, Chen YN, Campbell A, Sudha T, Yuan ZM, Narula J, Weichselbaum R, Nalin C, Kufe D (2000) Translocation of SAPK/JNK to mitochondria and interaction with Bcl-x(L) in response to DNA damage. *J Biol Chem* **275:** 322–327

Knudson CM, Tung KS, Tourtellotte WG, Brown GA, Korsmeyer SJ (1995) Bax-deficient mice with lymphoid hyperplasia and male germ cell death. *Science* **270:** 96–99

Krammer PH (2000) CD95's deadly mission in the immune system. *Nature* **407:** 789–795

Kuan CY, Yang DD, Samanta Roy DR, Davis RJ, Rakic P, Flavell RA (1999) The Jnk1 and Jnk2 protein kinases are required for regional specific apoptosis during early brain development. *Neuron* **22:** 667–676

Kuwana T, Mackey MR, Perkins G, Ellisman MH, Latterich M, Schneiter R, Green DR, Newmeyer DD (2002) Bid, Bax, and lipids cooperate to form supramolecular openings in the outer mitochondrial membrane. *Cell* **111:** 331–342

Lei K, Davis RJ (2003) JNK phosphorylation of Bim-related members of the Bcl2 family induces Bax-dependent apoptosis. *Proc Natl Acad Sci USA* **100:** 2432–2437

Lei K, Nimnual A, Zong WX, Kennedy NJ, Flavell RA, Thompson CB, Bar-Sagi D, Davis RJ (2002) The Bax subfamily of Bcl2-related proteins is essential for apoptotic signal transduction by c-Jun NH(2)-terminal kinase. *Mol Cell Biol* **22:** 4929–4942

Lindsten T, Ross AJ, King A, Zong WX, Rathmell JC, Shiels HA, Ulrich E, Waymire KG, Mahar P, Frauwirth K, Chen Y, Wei M, Eng VM, Adelman DM, Simon MC, Ma A, Golden JA, Evan G, Korsmeyer SJ, MacGregor GR, Thompson CB (2000) The combined functions of proapoptotic Bcl-2 family members bak and bax are essential for normal development of multiple tissues. *Mol Cell* **6:** 1389–1399

Liu D, Bienkowska J, Petosa C, Collier RJ, Fu H, Liddington R (1995) Crystal structure of the zeta isoform of the 14-3-3 protein. *Nature* **376:** 191–194

Masters SC, Pederson KJ, Zhang L, Barbieri JT, Fu H (1999) Interaction of 14-3-3 with a nonphosphorylated protein ligand, exoenzyme S of *Pseudomonas aeruginosa*. *Biochemistry* **38:** 5216–5221

Masuyama N, Oishi K, Mori Y, Ueno T, Takahama Y, Gotoh Y (2001) Akt inhibits the orphan nuclear receptor Nur77 and T-cell apoptosis. *J Biol Chem* **276:** 32799–32805

Maundrell K, Antonsson B, Magnenat E, Camps M, Muda M, Chabert C, Gillieron C, Boschert U, Vial-Knecht E, Martinou JC, Arkinstall S (1997) Bcl-2 undergoes phosphorylation by c-Jun N-terminal kinase/stress-activated protein kinases in the presence of the constitutively active GTP-binding protein Rac1. *J Biol Chem* **272:** 25238–25242

Molton SA, Todd DE, Cook SJ (2003) Selective activation of the c-Jun N-terminal kinase (JNK) pathway fails to elicit Bax activation or apoptosis unless the phosphoinositide 3′-kinase (PI3K) pathway is inhibited. *Oncogene* **22:** 4690–4701

Muslin AJ, Tanner JW, Allen PM, Shaw AS (1996) Interaction of 14-3-3 with signaling proteins is mediated by the recognition of phosphoserine. *Cell* **84:** 889–897

Nechushtan A, Smith CL, Hsu YT, Youle RJ (1999) Conformation of the Bax C-terminus regulates subcellular location and cell death. *EMBO J* **18:** 2330–2341

Nomura M, Shimizu S, Sugiyama T, Narita M, Ito T, Matsuda H, Tsujimoto Y (2003) 14-3-3 interacts directly with and negatively regulates pro-apoptotic Bax. *J Biol Chem* **278:** 2058–2065

Putcha GV, Deshmukh M, Johnson Jr EM (1999) BAX translocation is a critical event in neuronal apoptosis: regulation by neuroprotectants, BCL-2, and caspases. *J Neurosci* **19:** 7476–7485

Putcha GV, Le S, Frank S, Besirli CG, Clark K, Chu B, Alix S, Youle RJ, LaMarche A, Maroney AC, Johnson Jr EM (2003) JNK-mediated BIM phosphorylation potentiates BAX-dependent apoptosis. *Neuron* **38:** 899–914

Putcha GV, Moulder KL, Golden JP, Bouillet P, Adams JA, Strasser A, Johnson EM (2001) Induction of BIM, a proapoptotic BH3-only BCL-2 family member, is critical for neuronal apoptosis. *Neuron* **29:** 615–628

Sabapathy K, Kallunki T, David JP, Graef I, Karin M, Wagner EF (2001) c-Jun NH2-terminal kinase (JNK)1 and JNK2 have similar and stage-dependent roles in regulating T cell apoptosis and proliferation. *J Exp Med* **193:** 317–328

Saito M, Korsmeyer SJ, Schlesinger PH (2000) BAX-dependent transport of cytochrome *c* reconstituted in pure liposomes. *Nat Cell Biol* **2:** 553–555

Samuel T, Weber HO, Rauch P, Verdoodt B, Eppel JT, McShea A, Hermeking H, Funk JO (2001) The G2/M regulator 14-3-3sigma prevents apoptosis through sequestration of Bax. *J Biol Chem* **276:** 45201–45206

Sawada M, Sun W, Hayes P, Leskov K, Boothman DA, Matsuyama S (2003) Ku70 suppresses the apoptotic translocation of Bax to mitochondria. *Nat Cell Biol* **5:** 320–329

Shimizu S, Narita M, Tsujimoto Y (1999) Bcl-2 family proteins regulate the release of apoptogenic cytochrome *c* by the mitochondrial channel VDAC. *Nature* **399:** 483–487

Svennelid F, Olsson A, Piotrowski M, Rosenquist M, Ottman C, Larsson C, Oecking C, Sommarin M (1999) Phosphorylation of Thr-948 at the C terminus of the plasma membrane H(+)-ATPase creates a binding site for the regulatory 14-3-3 protein. *Plant Cell* **11:** 2379–2391

Tournier C, Hess P, Yang DD, Xu J, Turner TK, Nimnual A, Bar-Sagi D, Jones SN, Flavell RA, Davis RJ (2000) Requirement of JNK for stress-induced activation of the cytochrome *c*-mediated death pathway. *Science* **288:** 870–874

Tsujimoto Y, Shimizu S (2000) Bcl-2 family: life-or-death switch. *FEBS Lett* **466:** 6–10

Tsuruta F, Masuyama N, Gotoh Y (2002) The phosphatidylinositol 3-kinase (PI3K)-Akt pathway suppresses Bax translocation to mitochondria. *J Biol Chem* **277:** 14040–14047

van Hemert MJ, Steensma HY, van Heusden GP (2001) 14-3-3 proteins: key regulators of cell division, signalling and apoptosis. *BioEssays* **23:** 936–946

Wang X (2001) The expanding role of mitochondria in apoptosis. *Genes Dev* **15:** 2922–2933

Wei MC, Zong WX, Cheng EH, Lindsten T, Panoutsakopoulou V, Ross AJ, Roth KA, MacGregor GR, Thompson CB, Korsmeyer SJ (2001) Proapoptotic BAX and BAK: a requisite gateway to mitochondrial dysfunction and death. *Science* **292:** 727–730

Whitfield J, Neame SJ, Paquet L, Bernard O, Ham J (2001) Dominant-negative c-Jun promotes neuronal survival by reducing BIM expression and inhibiting mitochondrial cytochrome *c* release. *Neuron* **29:** 629–643

Wolter KG, Hsu YT, Smith CL, Nechushtan A, Xi XG, Youle RJ (1997) Movement of Bax from the cytosol to mitochondria during apoptosis. *J Cell Biol* **139:** 1281–1292

Xia Z, Dickens M, Raingeaud J, Davis RJ, Greenberg ME (1995) Opposing effects of ERK and JNK-p38 MAP kinases on apoptosis. *Science* **270:** 1326–1331

Xiao B, Smerdon SJ, Jones DH, Dodson GG, Soneji Y, Aitken A, Gamblin SJ (1995) Structure of a 14-3-3 protein and implications for coordination of multiple signalling pathways. *Nature* **376:** 188–191

Yaffe MB (2002) How do 14-3-3 proteins work? Gatekeeper phosphorylation and the molecular anvil hypothesis. *FEBS Lett* **513:** 53–57

Yaffe MB, Rittinger K, Volinia S, Caron PR, Aitken A, Leffers H, Gamblin SJ, Smerdon SJ, Cantley LC (1997) The structural basis for 14-3-3:phosphopeptide binding specificity. *Cell* **91:** 961–971

Yamaguchi H, Wang HG (2001) The protein kinase PKB/Akt regulates cell survival and apoptosis by inhibiting Bax conformational change. *Oncogene* **20:** 7779–7786

Yang DD, Kuan CY, Whitmarsh AJ, Rincon M, Zheng TS, Davis RJ, Rakic P, Flavell RA (1997) Absence of excitotoxicity-induced apoptosis in the hippocampus of mice lacking the Jnk3 gene. *Nature* **389:** 865–870

Yuan J, Yankner BA (2000) Apoptosis in the nervous system. *Nature* **407:** 802–809

Zha J, Harada H, Yang E, Jockel J, Korsmeyer SJ (1996) Serine phosphorylation of death agonist BAD in response to survival factor results in binding to 14-3-3 not BCL-X(L). *Cell* **87:** 619–628

Zhang L, Chen J, Fu H (1999) Suppression of apoptosis signal-regulating kinase 1-induced cell death by 14-3-3 proteins. *Proc Natl Acad Sci USA* **96:** 8511–8515

Zong WX, Lindsten T, Ross AJ, MacGregor GR, Thompson CB (2001) BH3-only proteins that bind pro-survival Bcl-2 family members fail to induce apoptosis in the absence of Bax and Bak. *Genes Dev* **15:** 1481–1486

Involvement of caspase-4 in endoplasmic reticulum stress-induced apoptosis and Aβ-induced cell death

Junichi Hitomi,[1,6] Taiichi Katayama,[1,6] Yutaka Eguchi,[2,6,7] Takashi Kudo,[3] Manabu Taniguchi,[1,6] Yoshihisa Koyama,[1,6] Takayuki Manabe,[1,6] Satoru Yamagishi,[1,6] Yoshio Bando,[4] Kazunori Imaizumi,[5] Yoshihide Tsujimoto,[2,6,7] and Masaya Tohyama[1,6]

[1]Department of Anatomy and Neuroscience, [2]Division of Molecular Genetics, and [3]Division of Psychiatry and Behavioural Proteomics, Department of Post-Genomics and Diseases, Graduate School of Medicine, Osaka University, Suita, Osaka 565-0871, Japan
[4]Department of Anatomy, Asahikawa Medical College, Midorigaoka Higashi, Asahikawa, Hokkaido, 078-8510, Japan
[5]Division of Structural Cell Biology, Nara Institute of Science and Technology, Takayama, Ikoma, Nara 630-0101, Japan
[6]21st Century COE Program, Japan Society for the Promotion of Science, Chiyoda-ku, Tokyo 102-8471, Japan
[7]Solution Oriented Research for Science and Technology of Japan, Science and Technology Agency, Honcho 4-1-8, Kawaguchi, Saitama, 332-0012, Japan

Recent studies have suggested that neuronal death in Alzheimer's disease or ischemia could arise from dysfunction of the endoplasmic reticulum (ER). Although caspase-12 has been implicated in ER stress-induced apoptosis and amyloid-β (Aβ)–induced apoptosis in rodents, it is controversial whether similar mechanisms operate in humans. We found that human caspase-4, a member of caspase-1 subfamily that includes caspase-12, is localized to the ER membrane, and is cleaved when cells are treated with ER stress-inducing reagents, but not with other apoptotic reagents. Cleavage of caspase-4 is not affected by overexpression of Bcl-2, which prevents signal transduction on the mitochondria, suggesting that caspase-4 is primarily activated in ER stress-induced apoptosis. Furthermore, a reduction of caspase-4 expression by small interfering RNA decreases ER stress-induced apoptosis in some cell lines, but not other ER stress-independent apoptosis. Caspase-4 is also cleaved by administration of Aβ, and Aβ-induced apoptosis is reduced by small interfering RNAs to caspase-4. Thus, caspase-4 can function as an ER stress-specific caspase in humans, and may be involved in pathogenesis of Alzheimer's disease.

Introduction

Recently, it has been reported that some human diseases, such as Alzheimer's disease (AD), Parkinson's diseases, and cystic fibrosis, and neuronal damage by ischemia are related to stress acting on the ER, which leads to intraluminal accumulation of unfolded proteins (Katayama et al., 1999; Wigley et al., 1999; Imai et al., 2000, 2001; Nakagawa et al., 2000; Sato et al., 2001; Tamatani et al., 2001). Stress on the ER can be induced in vitro by depletion of calcium from the ER lumen, inhibition of asparagine N-linked glycosylation, reduction of disulfide bonds, expression of mutant proteins, and ischemia (Imaizumi et al., 2001). ER stress induces three major cellular responses: unfolded protein response (UPR), ER-associated degradation, and apoptosis. Cells exposed to ER stress can up-regulate genes encoding chaperones that facilitate the protein folding process in the ER and reduce overall translation (UPR; Harding et al., 1999; Kaufman, 2002; Forman et al., 2003), or enhance proteasomal degradation of misfolded ER protein in cytosol (Bonifacino and Weissman, 1998; Travers et al., 2000), to reduce the accumulation and aggregation of misfolded proteins, and relieve cells from the stress (Kozutsumi et al., 1988). On the other hand, excessive or long-termed ER stress results in apoptotic cell death, involving nuclear fragmentation,

Address correspondence to Taiichi Katayama, Dept. of Anatomy and Neuroscience, Graduate School of Medicine, Osaka University, Suita, Osaka 565-0871, Japan. Tel.: 81-6-6879-3221. Fax: 81-6-6879-3229. email: katayama@anat2.med.osaka-u.ac.jp; or Yutaka Eguchi, Division of Molecular Genetics, Dept. of Post-Genomics and Disease, Graduate School of Medicine, Osaka University, Suita, Osaka 565-0871, Japan. Tel.: 81-6-6879-3363. Fax: 81-6-6879-3369.
email: eguchi@gene.med.osaka-u.ac.jp

Key words: apoptosis; ER stress; caspase-4; Alzheimer's disease; amyloid-β

Abbreviations used in this paper: Aβ, amyloid-β; AD, Alzheimer's disease; ICE, interleukin-1β converting enzyme; RNAi, RNA interference; siRNA, small interfering RNA; TRAF2, tumor necrosis factor receptor–associated factor 2; UPR, unfolded protein response.

The Journal of Cell Biology, Volume 165, Number 3, May 10, 2004 347–356
http://www.jcb.org/cgi/doi/10.1083/jcb.200310015

condensation of chromatin, and shrinkage of the cell body (Imaizumi et al., 2001). Several mechanisms that activate apoptotic signaling pathways have been reported. For example, the UPR increases the transcription of CHOP/GADD153 (Brewer et al., 1997), which is closely associated with cell death (Zinszner et al., 1998), recruitment of tumor necrosis factor receptor–associated factor 2 (TRAF2) to activated IRE1α induces c-Jun NH_2-terminal kinase activation (Urano et al., 2000), or calpain activates downstream caspase cascade (Nakagawa and Yuan, 2000). However, little is known about the precise mechanisms to lead to ER stress-induced cell death in humans.

Activation of caspases, a family of cysteine proteases that cleave substrates at specific aspartate residues, is a central mechanism in the apoptotic cell death process (Salvesen and Dixit, 1997; Thornberry and Lazebnik, 1998). Most of apoptosis-inducing stimuli lead to release of cytochrome *c* from mitochondria, which binds to Apaf-1 to activate caspase-9 (Li et al., 1997; Zou et al., 1997), one of initiator caspases with a long pro-domain, and then the activated caspase-9 cleaves effector caspases (Li et al., 1997), including caspases 3 and 7 with a relatively short pro-domain, to activate them. Antiapoptotic Bcl-2 family proteins can rescue cells from apoptosis by protecting mitochondria to prevent cytochrome *c* release (Kluck et al., 1997; Yang et al., 1997). Several initiator caspases are known to be activated upstream of the mitochondrial dysfunction by specific apoptotic stimuli. For example, Fas stimulation can activate caspase-8 (Fernandes-Alnemri et al., 1996; Muzio et al., 1996), which cannot be inhibited by Bcl-2 (Scaffidi et al., 1998). Among 14 known caspases, caspase-12 seems to be involved in signaling pathways specific to ER stress-induced apoptosis (Nakagawa et al., 2000). Pro–caspase-12 is predominantly localized to the ER, and is specifically cleaved by ER stress. Furthermore, caspase-12–deficient mice show a reduced sensitivity to amyloid-β (Aβ), which is found in brains from Alzheimer's patients (Selkoe, 1986) and shown to cause neuronal cytotoxicity (Yankner et al., 1989). Based on these findings, caspase-12 has been suggested to play an important role in the pathogenesis of AD and to represent a potential target of treatment. However, caspase-12 has only been cloned in the mouse and rat so far, and therefore it is controversial whether similar mechanisms operate in humans (Katayama et al., 1999; Rao et al., 2001; Fischer et al., 2002).

Human genome sequence that is highly homologous to mouse caspase-12 has been identified at the locus within the caspase-1/interleukin-1β converting enzyme (ICE) genes cluster on chromosome 11q22.3 (Fischer et al., 2002), but the gene is interrupted by frame shift and premature stop codon, and also has amino acid substitution in the critical site for caspase activity (Fischer et al., 2002). Therefore, human caspase-12 seems to be lost, and the caspases that substitute for caspase-12 to be activated specifically by ER stress have not been identified in humans so far. We described here that human caspase-4 located within the caspase-1/ICE genes cluster shows similar characteristics to mouse caspase-12. The role of the caspase-4 in ER stress-induced apoptosis and Aβ-induced cell death will be discussed.

Results

Identification of caspase-4 as a gene homologous to caspase-12

To detect a caspase that was specifically involved in ER stress, we screened human colon cDNA libraries by the plaque hybridization method using the mouse caspase-12 gene as a probe. Human caspase-4 was cloned as the most homologous gene to mouse caspase-12, in agreement with the fact that both molecules belong to the caspase-1/ICE subfamily within the caspase family (Kamens et al., 1995; Lin et al., 2000). Although caspase-5, which has slightly less homology to caspase-12 (caspase-4: 48%; caspase-5: 45%), was also isolated, the screening process yielded much more caspase-4 clones than caspase-5. Because caspase-4 but not caspase-5 was expressed in the cell lines used in this work, which underwent apoptosis in response to ER stress, we assumed that human caspase-4 might functionally substitute for mouse caspase-12 in the human system, and further analyzed the possible role of caspase-4 as a mediator of ER stress-induced apoptosis.

Subcellular localization of caspase-4

First, we studied the subcellular localization of endogenous caspase-4 in SK-N-SH human neuroblastoma cells. Immunofluorescence microscopy showed that immunostaining pattern of caspase-4 strictly overlapped with that of ER markers such as GRP78 and GRP94 (Fig. 1, a–c). Immunoreactivity of caspase-4 was found to overlap only in part with fluorescence signals from Mitotracker (Fig. 1, d–f). These results suggest that caspase-4 was localized predominantly to the ER, and to the mitochondria in addition. The similar results were obtained using HeLa cells (Fig. 1, g–l). When caspase-4 fused with GFP at its COOH terminus was overexpressed in HeLa cells to see the subcellular localization in live cells, most of the fluorescent signals from caspase-4/GFP fusion protein overlapped with those from ER-tracker (Fig. 1, m–o), confirming predominant localization of caspase-4 to the ER by non-immunological method. The immunoelectron microscopic analysis showed that the immunoreactive signals for caspase-4 were found on the ER and mitochondria (Fig. 1, p–r), but much less signals on the nuclei (Fig. 1 r). We also performed biochemical fractionation analysis. Although we could not eliminate contamination of ER marker proteins in the mitochondria-enriched fraction using SK-N-SH cells, probably because we could not disrupt cells homogeneously as the cell line displays heterogeneity in cellular morphology, microsome-enriched fraction does not seem to contain mitochondria and cytosol (Fig. 1 s). Under these conditions, caspase-4 was recovered in both mitochondria-enriched fraction and microsome-enriched fraction, and in cytosolic fraction to a lesser extent (Fig. 1 s), indicating that caspase-4 was surely in microsome-enriched fraction. From these results, we concluded that caspase-4 was localized to the ER, and to the mitochondria in addition, in both SK-N-SH and HeLa cells.

Specific cleavage of caspase-4 by ER stress and Aβ treatments

To examine whether caspase-4 was specifically cleaved by ER stress, we analyzed the cleavage of pro–caspase-4 in re-

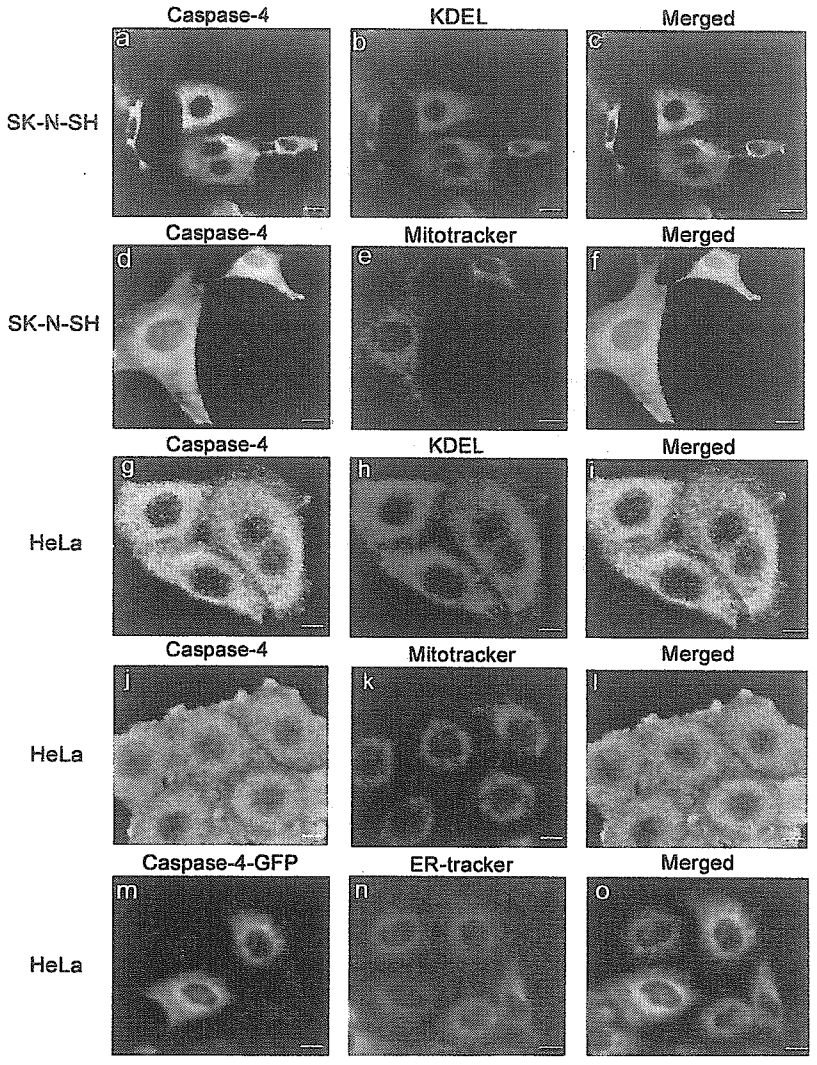

r

	Nuclear	Mitochondria	ER	Cytosol	total
Gold	0	359	392	169	920
%	0	39	43	18	100

s

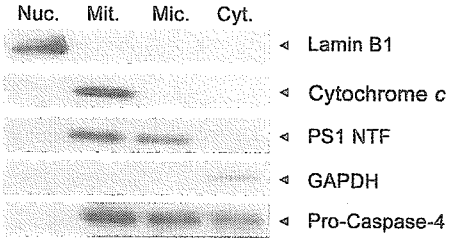

Figure 1. **Localization of caspase-4 in SK-N-SH and HeLa cells.** (a–l) SK-N-SH cells (a–f) or HeLa cells (g–l) were stained with anti–caspase-4 and anti-KDEL antibodies (a and g, caspase-4, green; b and h, KDEL, red; c and i, overlapping, yellow), or with anti–caspase-4 antibody and Mitotracker (d and j, caspase-4, green; e and k, Mitotracker, red; f and l, overlapping, yellow), and observed under a confocal microscope as described in Materials and methods. Anti-KDEL antibody detects both GRP78 and GRP94 (ER markers), whereas Mitotracker stains the mitochondria. (m–o) HeLa cells were transfected with a caspase-4–GFP fusion gene, and were stained with ER-tracker (m, caspase-4, green; n, ER-tracker, blue; o, overlapping, blue-green), and observed under a nonconfocal fluorescence microscope. Bars, 5 μm. (p and q) Immunoelectron microscopic analysis was performed for SK-N-SH cells as described in Materials and methods. Photograph shown in panel q is the enlarged image of a part of photograph p. Gold grains showed the immunoreactivity of caspase-4, and blue and red arrows showed the ER and mitochondria, respectively. Bars: (p) 200 nm; (q) 90 nm. (r) Gold grains observed on indicated organelles in immunoelectron microscopic analysis were counted and displayed. (s) Biochemical fractionation was performed as described in Materials and methods, and analyzed by Western blotting using the indicated antibodies. Lamin B1, nuclear marker; cytochrome *c*, mitochondrial marker; presenilin-1 NH_2-terminal fragment (PS1 NTF), microsomal marker; and glyceraldehyde-3-phosphate dehydrogenase (GAPDH), cytosolic marker.

sponse to several apoptotic stimuli (Fig. 2 a). We found that cleavage of pro–caspase-4 was induced in SK-N-SH cells by treatment with tunicamycin and thapsigargin, both of which caused ER stress. In contrast, when cells were exposed to non-ER stress inducers such as etoposide, staurosporine, and UV at a dose providing similar extent of cell death to that by tunicamycin and thapsigargin, final cleavage products of pro–caspase-4 (Fig. 2 a, cleaved-caspase-4, arrowhead) was not observed. Although the bands shown by the asterisks in Fig. 2 a, which should be derived from pro–caspase-4 by unknown processing reaction, judging from the data below (Fig. 4 b), were also increased, they were also observed in nontreated cells, so we speculated that the bands were not the final processed form of caspase-4. Under the same conditions, cleavage of caspases 3 and 7, the downstream caspases, was observed regardless of apoptotic stimulations (Fig. 2 a). These results suggest that caspase-4 is specifically activated by apoptotic stimuli inducing ER stress, but not by other stimuli that do not cause ER stress.

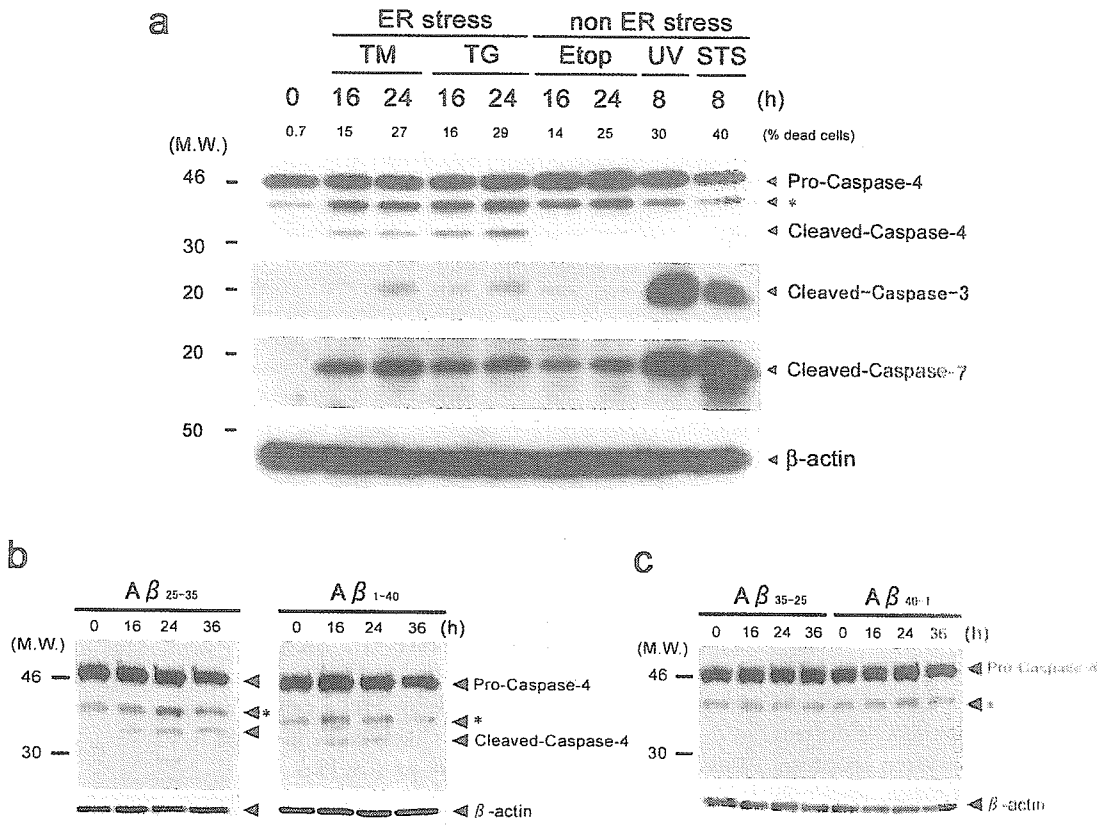

Figure 2. **Specific cleavage of caspase-4 by ER stress and Aβ treatment.** (a) SK-N-SH cells were treated with 1 μg/ml tunicamycin (TM), 0.5 μM thapsigargin (TG), 100 μM etoposide (Etop), or 0.1 μM staurosporine (STS) for indicated periods, or irradiated with 150 J/m^2 UV followed by incubation for indicated periods. Equal amounts of cell lysates (15 μg) were analyzed by Western blotting using anti–caspase-4 antibody (top), anti–caspase-3 antibody (second from top), anti–caspase-7 antibody (third from top), or anti–β-actin antibody (bottom). Positions of pro–caspase-4, cleaved caspase-4, cleaved caspase-3, cleaved caspase-7, and β-actin are indicated. Extent of cell death assessed by MTS assay after incubation for indicated periods are also shown at the top of the gels. (b) SK-N-SH cells were treated with 25 μM synthetic $A\beta_{25\text{-}35}$ or 5 μM $A\beta_{1\text{-}40}$ peptides for the indicated periods. Equal amounts of cell lysates (15 μg) were analyzed by Western blotting using anti–caspase-4 antibody (top) and anti–β-actin antibody (bottom) as a control. Positions of pro–caspase-4, cleaved caspase-4, and β-actin are indicated. (c) SK-N-SH cells were treated with the reverse peptides (25 μM $A\beta_{35\text{-}25}$ and 5 μM $A\beta_{40\text{-}1}$, respectively) for the indicated periods, and cleavage of caspase-4 was examined as in panel b. (a–c) Bands marked by asterisks are likely to be derived from pro–caspase-4 by unknown processing reaction.

To address the possibility that caspase-4 contributes to the mechanism of Aβ-induced cell death in humans, we examined the cleavage of caspase-4 in SK-N-SH cells after treatment with Aβ. When cells were incubated with 25 μM $A\beta_{25\text{-}35}$ or 5 μM $A\beta_{1\text{-}40}$, cleavage of caspase-4 was observed (Fig. 2 b). In contrast, treatment of cells with the reverse peptides ($A\beta_{35\text{-}25}$ and $A\beta_{40\text{-}1}$, respectively), which were not toxic, did not induce the cleavage of caspase-4 (Fig. 2 c). These results suggest that caspase-4 is activated by neurotoxic Aβ treatment similar to ER stress-induced apoptosis.

Cleavage of caspase-4 in the presence of Bcl-2

To confirm that cleavage of caspase-4 was not due to other caspases activated downstream of the mitochondrial pathway, we examined the effect of overexpression of Bcl-2 and Bcl-x_L on apoptosis induced by tunicamycin. Apoptotic nuclear morphological changes were induced by treatment of vector transfectants of SK-N-SH and of HeLa cells with tunicamycin for 30 h, but such changes were completely suppressed by overexpression of Bcl-2 (Fig. 3) or Bcl-x_L (not depicted), indicating that the apoptotic signaling pathway downstream of mitochondria was not operating in cells with overexpression of these antiapoptotic proteins. However, cleavage of caspase-4 after 16 h of tunicamycin treatment was only slightly affected by overexpression of Bcl-2 (Fig. 3) or Bcl-x_L (not depicted). These results suggested that caspase-4 is largely activated before the activation of effector caspases during ER stress-induced cell death.

Requirement of caspase-4 for ER stress- and Aβ-induced apoptosis

To determine whether caspase-4 is required for ER stress-induced cell death, SK-N-SH cells that expressed endogenous caspase-4 were transfected with small interfering RNA (siRNA) to caspase-4 or GFP as a control. Immunofluorescence analysis showed that the amount of caspase-4 was substantially decreased by incubation for 60 h after transfection with siRNA directed against caspase-4, but immunoreactivity of caspase-4 was not affected by transfection with GFP-siRNA, when compared with nontransfected cells (Fig. 4 a). Western blot analysis also showed that the amount of caspase-4 was decreased by siRNA to caspase-4 (Fig. 4 b). These re-

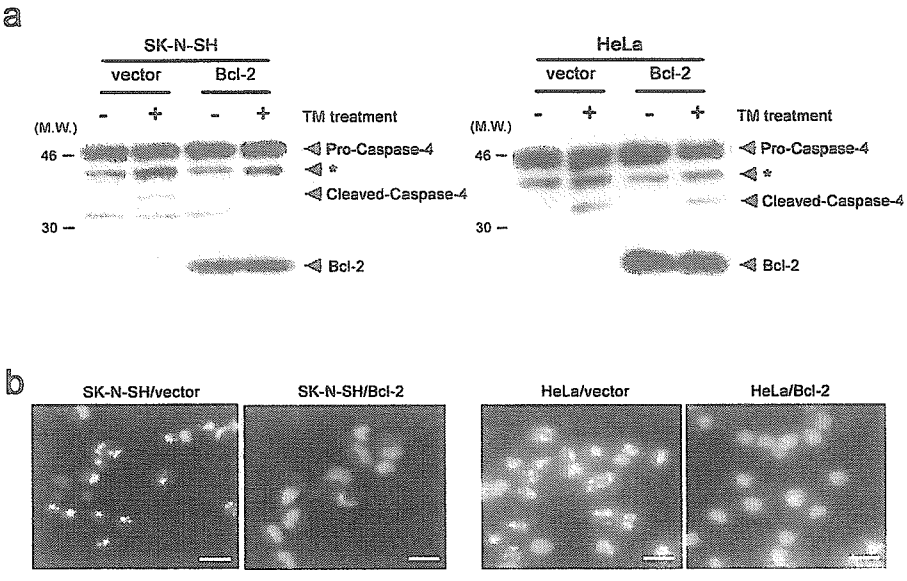

Figure 3. **No effect of Bcl-2 overexpression on ER stress-induced cleavage of caspase-4.** (a) SK-N-SH cells (left) and HeLa cells (right) stably transfected with the vector or a Bcl-2 expression system were incubated with (+) or without (−) 1 μg/ml tunicamycin for 16 h. Equal amounts of cell lysates were analyzed by Western blotting using anti–caspase-4 antibody (top) and anti–Bcl-2 antibody (bottom). Positions of pro–caspase-4, cleaved caspase-4, and Bcl-2 are indicated. Asterisks show processed caspase-4 as described in Fig. 2 a. (b) The indicated cells were treated with 1 μg/ml tunicamycin for 30 h, stained with Hoechst 33342, and observed under a fluorescence microscope. Bars, 25 μm.

sults showed that the siRNA could diminish the amount of caspase-4, and that the antibody used here specifically recognized caspase-4 in immunohistochemical analysis.

We next examined the effect of decrease in caspase-4 level by siRNA on ER stress-induced apoptosis. Assessment of cell death on the basis of morphological changes showed that ~60% of untransfected SK-N-SH cells were killed by treatment with thapsigargin for 40 h. The extent of cell death was unaffected by transfection with siRNA to GFP (Fig. 4 c). In contrast, only ~30% of the cells died after being transfected with caspase-4 siRNA and exposed to the same stimulation with thapsigargin (Fig. 4 c). As shown in Fig. 4 b, treatment with thapsigargin for 24 h yielded lower level of cleaved-caspase-4 in the cells transfected with caspase-4 siRNA than in the cells transfected with GFP-siRNA. Because the amount of cleaved caspase-4 shown in Fig. 4 b seemed to correlate with the extent of cell death in Fig. 4 c, incomplete inhibition of cell death by transfection with caspase-4 siRNA could be due to residual activity of caspase-4. These results indicate that cells with decreased expression of caspase-4 become more resistant to ER stress-induced cell death.

When cell death was examined by the MTS assay, treatment with caspase-4 siRNA, but not with GFP-siRNA, increased the resistance to ER stress-induced cell death (Fig. 4 d). The increase in the resistance to ER stress-induced cell death was also observed when siRNA to caspase-4 with a different sequence (caspase-4 siRNA-b) was used (Fig. 4 d), indicating that the effect was due to the decreased expression of caspase-4, but not by a specific side effect of caspase-4 siRNA that might affect the expression of other genes. On the other hand, the efficiency of cell death induced by etoposide treatment was not significantly affected by both caspase-4 siRNAs (Fig. 4 d). Therefore, caspase-4 is likely to be specifically involved in ER stress-induced cell death.

To know whether caspase-4 is involved in ER stress-induced cell death in other cell lines, we examined the effect of caspase-4 siRNA using HeLa cells. As shown in Fig. 4 e, treatment of HeLa cells with caspase-4 siRNA significantly increased the resistance to ER stress-induced cell death, although the extent of the increase in resistance was less than that observed for SK-N-SH cells. This is probably because some other apoptotic mechanisms might also operate simultaneously in HeLa cells. Therefore, we concluded that caspase-4 is likely to be involved in ER stress-induced cell death at least in part in HeLa cells.

We next examined whether caspase-4 is involved in Aβ-induced cell death. When treated with $A\beta_{25\text{-}35}$, SK-N-SH cells transfected with caspase-4 siRNA showed significant reduction in cell death compared with the cells transfected with GFP-siRNA (Fig. 4 f). From these results presented here, we concluded that caspase-4 is involved in Aβ-induced cell death, as well as in ER stress-induced cell death.

Discussion

It has been known that apoptotic morphological changes are observed in cell death caused by ER stress (Imaizumi et al., 2001). Caspases are activated to transmit apoptotic signals transcending the difference in species (Alnemri et al., 1996). In rodents, caspase-12 mediates apoptosis specifically in response to ER stress (Nakagawa et al., 2000). Although human caspase-12 gene is transcribed into mRNA, mature caspase-12 protein would not be produced, because the gene is interrupted by frame shift and premature stop codon (Fischer et al., 2002). Furthermore, it contains amino acid substitution in the critical site, which leads to loss of function in several caspases (Fischer et al., 2002). Thus, human caspase-12 does not seem to function in ER stress-induced apoptosis, and some other caspases with similar structure might substitute functionally for caspase-12 in humans. The caspase-12 gene is located within a region where caspase-1/ICE subfamily genes cluster (caspases 1, 4, 5, 12 in human and caspases 1, 11, 12 in mouse). No locus with a comparably high homology to rodent caspase-12 could be found in the human genome. Caspases 4 and 5 are located between caspases 1 and 12 in human genome, whereas only caspase-11 is located between caspases 1 and 12 in mouse. Although it is not known why the region in human genome contains gene duplication, caspases 4 and 5 have been thought to function similarly to caspases 11 and 12. Mouse caspase-11